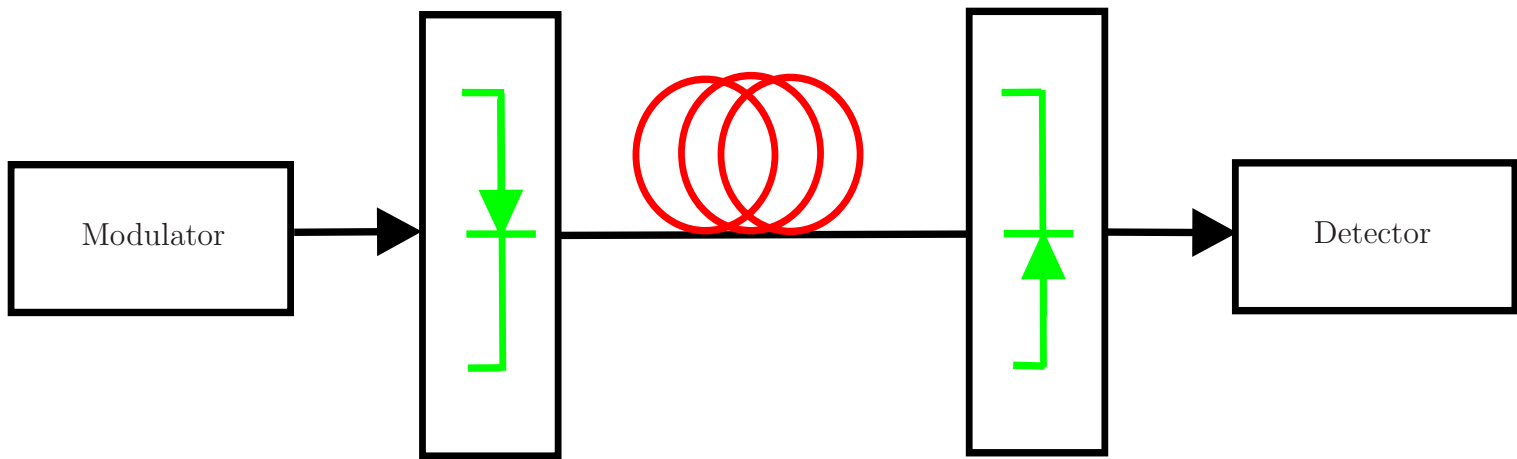# CHALMERS



# BANDLIMITED INTENSITY MODULATION

### MEHRNAZ TAVAN

*Communication Systems Group*

*Department of Signals and Systems*

CHALMERS UNIVERSITY OF TECHNOLOGY

Göteborg, Sweden                               EX047/2012

Tavan, Mehrnaz

Bandlimited Intensity Modulation

Department of Signals and Systems

Technical Report N0. EX047/2012

Communication Systems Group

Department of Signals and Systems

Chalmers University of Technology

SE-412 96 Göteborg, Sweden

Telephone: + 46 (0)31-772 1000

This thesis has been prepared using LaTeX.

Cover: [An abstract representation of an intensity-modulated direct-detection (IM/DD) system. The green object in the left represent light source, whereas the one in the right indicates photodetector. The red circles in the center are the symbols of optical link.]

# Abstract

In this paper, the design and analysis of a new bandwidth-efficient signaling method over the bandlimited intensity-modulated direct-detection (IM/DD) channel is presented. The channel can be modeled as a bandlimited channel with nonnegative input and additive white Gaussian noise (AWGN). Due to the nonnegativity constraint, standard methods for coherent bandlimited channels cannot be applied here. Previously established techniques for the IM/DD channel require bandwidth twice the required bandwidth over the conventional coherent channel. We propose a method to transmit without intersymbol interference in a bandwidth no larger than the bit rate. This is done by combining Nyquist or root-Nyquist pulses with a constant bias and using higher-order modulation formats. In fact, we can transmit with a bandwidth equal to that of coherent transmission. A trade-off between the required average optical power and the bandwidth is investigated. Depending on the bandwidth required, the most power-efficient transmission is obtained by the parametric linear pulse, the so-called "better than Nyquist" pulse, or the root-raised cosine pulse.

KEYWORDS: Indoor diffuse wireless optical communications, intensity-modulated direct-detection (IM/DD), matched filter, Nyquist pulses, optical communications, root-Nyquist pulses, short-haul optical fiber links, strictly bandlimited signaling.

# Preface

This report is the result of conducting a one-year 60 credit thesis work which is the requirement for obtaining Master of Science degree. This work is an extended version of M. Tavan, E. Agrell, and J. Karout, "Bandlimited intensity modulation," to appear in IEEE Transactions on Communications, 2012, which in turn is an extended version of M.Tavan, E. Agrell, and J. Karout, "Strictly bandlimited ISI-free transmission over intensity-modulated channels," in Proceedings of Global Communications Conference (GlobeCom), Houston, TX, Dec. 2011.

September 7, 2012

Mehrnaz Tavan

# Acknowledgements

# GLOSSARY

*Notations*

| | |
|---|---|
| $A$ | scaling factor |
| $a$ | information symbol |
| $B$ | lowpass bandwidth |
| $\mathcal{C}$ | finite set of constellation points |
| $C_n$ | Fourier series coefficient |
| $\mathbb{E}\{\cdot\}$ | expectation |
| $E_q$ | pulse energy |
| $f_{\mathrm{c}}$ | optical carrier frequency |
| $G(\omega)$ | receiver filter frequency response |
| $g(t)$ | receiver filter impulse response |
| $h(t)$ | channel impulse response |
| $I(t)$ | electrical signal |
| $J$ | laser conversion factor |
| $L$ | constellation offset |
| $M$ | number of levels in the modulation |
| $N_0/2$ | double-sided power spectral density of noise |
| $n(t)$ | noise at the receiver |
| $O(t)$ | optical signal |
| $P_{\mathrm{err}}$ | bit error probability |
| $P_{\mathrm{opt}}$ | average optical power |
| $P_{\mathrm{max}}$ | maximum optical power |
| $Q(\omega)$ | Fourier transform of $q(t)$ |
| $q(t)$ | arbitrary pulse |
| $R$ | responsivity of the photodetector |
| $r(t)$ | output of the receiver filter |
| $T_{\mathrm{s}}$ | symbol duration |

$T_\mathrm{b}$     bit duration

$u(t)$     noise at the output of matched filter receiver

$x(t)$     intensity of the optical signal

$y(t)$     received electrical signal

$z(t)$     noise at the output of sampling receiver

*Subscripts*

$k$     discrete time instant

opt    optical

ref     reference system

*Superscripts*

ref    reference system

\*     complex conjugate

*Abbreviations*

AB-QAM    Adaptively Biased QAM

ADR         Asymptotic Decay Rate

AWGN      Additive White Gausian Noise

BPSK       Binary Phase-Shift Keying

BTN         Better Than Nyquist

DC          Direct-Current

DJ          Double-Jump

DPPM      Differential PPM

FTTH       Fiber to the Home

IM/DD     Intensity-Modulated Direct-Detection

ISI          Intersymbol Interference

LAN         Local Area Network

| | |
|---|---|
| LED | Light-Emitting Diode |
| MF | Matched Filter Receiver |
| MSM | Multi Subcarrier Modulation |
| OFDM | Orthogonal Frequency Division Multiplexing |
| OOK | On-Off Keying |
| PAM | Pulse-Amplitude Modulation |
| PL | Parametric Linear |
| Poly | Polynomial |
| PPM | Pulse Position Modulation |
| PSK | Phase-Shift Keying |
| QAM | Quadrature Amplitude Modulation |
| RC | Raised-Cosine |
| RRC | Root-Raised Cosine |
| S | Sampling Receiver |
| S2 | Squared Sinc |
| SDJ | Squared DJ |
| SER | Symbol Error Rate |
| SRC | Squared Raised-Cosine |

*Greek Letters*

| | |
|---|---|
| $\alpha$ | roll-off factor |
| $\zeta$ | matched filter gain |
| $\theta$ | random phase of optical signal |
| $\mu$ | required DC bias |

$\sigma^2$    noise variance

$\Delta$    minimum distance between constellation points

$\Upsilon$    optical power gain

*Diacritical marks*

ˆ    maximum

¯    average

˘    minimum

$\otimes$    convolution

# CONTENTS

# 1 INTRODUCTION

The growing demand for high-speed data transmission systems has introduced new design paradigms for optical communications. The need for low-complexity and cost-effective systems has motivated the usage of affordable optical hardware (e.g., incoherent transmitters, optical intensity modulators, multimode fibers, direct-detection receivers) to design short-haul optical fiber links (e.g., fiber-to-the-home and optical interconnects) [1, 2] and diffuse indoor wireless optical links [3–5]. These devices impose three important constraints on the signaling design:

- First, the transmitter only modulates information on the instantaneous intensity of an optical carrier, contrary to conventional coherent channels where the amplitude and phase of the carrier can be used to send information [6, Sec. 4.3]. In the receiver, only the optical intensity of the incoming signal will be detected [4] since the output of detector is an electrical current which is proportional to the detected intensity. Due to these limitations, the transmitted signal must be nonnegative. Such transmission is called intensity modulation with direct detection (IM/DD).

- Second, the peak and average optical power (i.e., the peak and average of the transmitted signal in the electrical domain) must be below a certain threshold for eye- and skin-safety concerns [4] and to avoid nonlinearities present in the devices [7, 8]. In conventional channels, such constraints are usually imposed on the peak and average of the squared electrical signal.

- Third, the bandwidth is limited due to the impairments in the optoelectronic devices [5, 9] and other limitations (e.g., modal dispersion in short-haul optical fiber links [10] and multipath distortion in diffuse indoor wireless optical links [4]). Consequently, the coherent modulation formats and pulse shaping

methods designed for conventional electrical channels (i.e., with no nonneg-
ativity constraint on the transmitted signal) cannot be directly applied to
IM/DD channels.

## 1.1    Thesis Contributions

In this study, we present a new signaling method for bandlimited IM/DD channels,
in which the transmitted signal becomes nonnegative by the addition of a constant
direct-current (DC) bias. This method provides us with two benefits: (i) We can
transmit with no intersymbol interference (ISI) with a bandwidth equal to that of
coherent conventional channels, while benefiting from the reduced complexity and
cost of IM/DD system. (ii) We can implement the system using either Nyquist pulses
with sampling receiver or root-Nyquist pulses with matched filter receiver. By being
able to use a larger variety of pulses, the transmitted power can be reduced compared
with known methods, which is advantageous in power-sensitive optical interconnects
and indoor wireless optical links. We also evaluate the spectral efficiency and optical
power efficiency of binary and 4-PAM formats with Nyquist and root-Nyquist pulses
for achieving a specific noise-free eye opening or a specific symbol-error-rate (SER).

## 1.2    Organization of the Thesis

The remainder of the report is organized as follows. Chapter 2 gives a brief overview
of the previous works that has been done about bandlimited signaling in conven-
tional and intensity modulated channels and investigates various modulation for-
mats. Chapter 3 presents the system model. In Chapter 4, after giving the criteria
in selecting the proper pulse, we define the Nyquist pulses that have been used ex-

tensively for conventional bandlimited channels, as well as the ones that have been suggested for nonnegative bandlimited channels. Moreover, the root-Nyquist pulses used in this study are introduced. Chapter 5 discusses a method of computing the required DC bias for a general pulse. Chapter 6 introduces the performance measures and analyzes the performance of the system under different scenarios. Finally, conclusions are drawn in Chapter 7 on the performance of the system.

# 2 PREVIOUS WORKS

## 2.1 Conventional Channels

Modern communication systems aim at increasing the amount of data transmitted over the channel and decreasing the probability of error simultaneously [11–13]:

- To increase the amount of transmitted data without any need to increase the bandwidth, multilevel modulation formats have been used [14]. One of the main drawbacks with multilevel modulation formats is the power consumption which increases significantly by increasing the level of the modulation. To solve this problem, the data is modulated on both phase and amplitude of the carrier using coherent transmitters and detectors. However, this type of transmission (coherent transmission) requires the phase of the signal to be detected at the receiver which increases the complexity. In coherent optical applications, the transmitter requires a narrow-band laser and an external modulator (Mach Zehnder modulator (MZM)), and the receiver needs a local oscillator laser, and more advanced devices [15].

- To decrease the error probability, the received samples should not have large ISI. Using Nyquist criteria, proper pulses which do not create ISI at periodic sampling instants can be designed [6, Eq. (9.2-11)]. Pulse shaping for the purpose of reducing ISI in conventional channels has been previously investigated in [6, Sec. 9], [11–13, 16–18].

## 2.2 Intensity-Modulated Direct-Detection channels

Depending on the devices used in the link, there are three types of optical communication systems: (i) Coherent detection systems which have similar shaping techniques to the coherent conventional channels [19]. (ii) Intensity-modulated direct-detection (IM/DD) systems without optical amplifiers, which are analyzed in this study. Such systems can be modeled with nonnegative transmitted signal and additive white Gaussian noise (AWGN). As a result, in contrast to previous case, the shaping methods for coherent transmission cannot be applied directly [20].(iii) IM/DD systems with optical amplifiers which are used in long-haul and metropolitan fiber systems. The only difference with (IM/DD) is that the dominant noise source is signal-spontaneous beat noise, which is signal-dependent [21].

In applications such as diffuse indoor wireless optical links [22, 23] and short-haul optical fiber communications [1, 2], where inexpensive hardware is used, IM/DD is often employed. In such systems, the data is modulated on the optical intensity of the transmitted light using an optical intensity modulator such as a laser diode or a light-emitting diode (LED). This optical intensity is proportional to the transmitted electrical signal. As a result, the transmitted electrical signal must be nonnegative. This is in contrast to conventional electrical channels, where the data is modulated on the amplitude and phase of the carrier [6, Sec. 4.3]. In the receiver, the direct-detection method is used in which the photodetector generates an output which is proportional to the incident received instantaneous power [24]. Another limitation, which is considered for safety purposes, is a constraint on the peak and average optical power, or equivalently, a constraint on the peak and average of the signal in the electrical domain [4, 9, 25–27]. Consequently, the methods designed for coherent conventional transmission cannot be directly applied here. Much research has been conducted on determining upper and lower bounds on the capacity of IM/DD

channels considering power and bandwidth limitations [25–30].

## 2.2.1   Time-Limited Signaling

Many studies have analyzed the time-limited signaling design for IM/DD channels. In [4, 24, 31–36], the performance of various modulation formats in IM/DD channels were studied using rectangular or other time-disjoint (i.e., infinite-bandwidth) pulses. Specifically, these pulses are used with $M$-ary pulse-amplitude modulation [4,37,38] and $M$-ary pulse-position modulation ($M$-PPM) [22, Sec. 5.3.3] [4,5,37,38] (which is more power efficient while requiring additional bandwidth).

To be able to use more variety of multi-level modulation formats (e.g., $M$-ary phase-shift keying ($M$-PSK) or $M$-ary quadrature amplitude modulation ($M$-QAM)), sub-carrier modulation method [22, Ch. 5] [39–41] is employed. In this method, the data is initially modulated using any two-dimensional modulation format. The lowest possible subcarrier frequency that can be used in this stage, while maintaining orthogonality between the in-phase and quadrature components, is equal to the symbol rate. To make the signal nonnegative, a DC bias is added. Finally, the signal will be modulated to the optical carrier frequency. Most of the operations including modulation are done in electrical domain (i.e., baseband part of the system) which reduces the complexity of the devices. Since this method performs an initial modulation to an electrical subcarrier frequency before modulation to the optical frequency, the required bandwidth is more than that of the $M$-ary pulse amplitude modulation ($M$-PAM) [22, p. 125]. In the receiver, after converting the signal from optical frequency to subcarrier frequency, conventional detection methods are used. In [34], it is shown that to make the signal nonnegative for QAM format over IM/DD channel, the constellation points must be within an infinite cone, with apex angle equal to $\cos^{-1}(1/3) = 70.5°$.

We can superimpose a large number of the subcarriers used to modulate information to create multiple-subcarrier modulation (MSM) [22, p. 122] [33], and orthogonal frequency-division multiplexing (OFDM) if the carriers are orthogonal [42]. MSM is not power efficient since the peak-to-average power ratio is high in these systems. [4] has proved that MSM schemes require several decibels more optical power than on-off keying (OOK). Moreover, the interference between subcarriers and multipath distortion (since multipath channels are lowpass) [4, 33] increases the amount of required power. OFDM is widely used in conventional channels to reduce ISI caused by multipath transmission or by a dispersive channel [43]. The OFDM requires a large DC bias to become nonnegative [5, 33, 44, 45] since in MSM systems, large negative amplitude may occur. As a result, systems using OFDM will suffer from large optical power. To solve this problem, asymmetrically clipped optical OFDM signals (ACO-OFDM) are used which have been shown to be more efficient in terms of optical power than OOK and PPM [46]. Alternatively, [47] designed optimized block codes to reduce average optical power in MSM systems.

In all the mentioned methods which use DC bias to become nonnegative, to improve the power efficiency, the bias can carry information. [24,48] changes the DC bias on a symbol-by-symbol basis to reduce optical power consumption and improve detection. [47] changes the DC bias within the symbol interval. In [44] the constellation points are assigned to subcarriers in a given symbol such that the average optical power will be low and minimum distance between each pair of codewords is maximized. [49] adds carriers at high frequencies outside of the data transmission bandwidth of the channel to reduce the average optical power.

## 2.2.2 Bandwidth-Limited Signaling

In most of the previous studies, as explained in Sec. 2.2.1, the bandwidth constraint of the channel was ignored in signaling design. Previous studies mostly concentrated

on spectrally efficient signaling using rectangular pulse sets [4, 24, 31, 32]. Wider classes of time-limited pulse sets have also been considered in [33, 34]. Using such pulses creates problems specially for the applications where having a large bandwidth will cause multipath distortion or other impairments. [5] presents an overview of the bandwidth efficient modulation schemes for indoor wireless optical links. However, in all the aforementioned works, strictly time-limited pulses are considered and none of these references has worked on strictly bandlimited pulses.

Hranilovic in [50] pioneered in investigating the problem of designing strictly bandlimited pulses for IM/DD channels with nonnegative PAM schemes. Unlike previous works, he did not restrict his work to time-limited pulses. He showed the existence of nonnegative bandlimited Nyquist pulses, which can be used for ISI-free transmission over IM/DD channels, and evaluated the performance of such pulses. He proved that the pulses that satisfy all three constraints (i.e., being nonnegative, bandlimited, and Nyquist) must be square of a Nyquist pulse. He also showed that any nonnegative root-Nyquist pulse must be time limited to a single symbol interval (i.e., infinite bandwidth). In other words, amplitude nonnegativity constraint of optical intensity channels eliminates the possibility of finding bandlimited nonnegative root-Nyquist pulses. Hence receivers with matched filters are not suitable for Hranilovic's signaling method. He concluded that transmission is possible with a bandwidth twice the required bandwidth over the corresponding conventional electrical channels. This work was extended to other Nyquist pulses that can introduce a trade-off between bandwidth and average optical power in [9, 51]. In other words, pulses with excess bandwidth are introduced that are more power efficient. Moreover, he investigated a family of bandwidth-efficient nonnegative root-Nyquist pulses called prolate spheroidal wave functions. These pulses have the lowest bandwidth among all time-limited functions [52], and might be a good substitute for other time-limited pulses [9].

## 2.3   Overview of Different Modulation Formats

### 2.3.1   On-Off Keying (OOK)

On-off keying (OOK) is one of the simplest modulation schemes. In OOK, there are two levels for data transmission (zero and one), so the presence and absence of signal each represents a symbol. OOK is often used for IM/DD channels since it is very power efficient and simple. However, it uses more bandwidth compared to multilevel modulation formats at the same bitrate.

### 2.3.2   $M$-ary Pulse-Amplitude Modulation ($M$-PAM)

In this modulation scheme, the amplitude of the pulse obtains one of the $M$ levels depending on the input symbol. This scheme is widely used over indoor optical channels [4]. [53] conducts an analysis of the 4-PAM IM/DD link. The advantage with this scheme is that we can transmit $\log_2 M$ bits per each transmitted symbol, so it reduces the required bandwidth compared to binary modulation schemes. However, since the level of the signal increases, the required power increases compared to binary schemes. We have made minor changes in the design of $M$-PAM so it can be used in noncoherent transmission.

### 2.3.3   $M$-ary Pulse-Position Modulation ($M$-PPM)

In this modulation scheme, each symbol period is divided into several intervals (chips). Depending on the transmitted symbol, a pulse is transmitted in one of the chips, while other chips have zero amplitude. In other words, the transmitted symbol is modulated on the position of the chip in symbol period. In PPM, all signals are orthogonal and have equal energy. Since $M$-PPM requires time-limited

pulses, it is not suitable for a bandlimited system. Consequently, we have not used it in our problem.

Overlapping-PPM (OPPM), is a variation of PPM which is used widely in IM/DD systems and allows overlap between adjacent pulse-positions and requires less bandwidth compared to PPM [37, 54–56]. In [57, 58], it is shown that to maximize the SNR, a binary modulation format is designed which consists of a zero pulse and a pulse which is nonzero only in a narrow part of the whole symbol period. The difference between this modulation format and OOK is that OOK is nonzero in the whole symbol period whereas this is nonzero only in a narrow part.

**Comparison of PPM and PAM**

Comparing PAM and PPM, it can be determined that PPM requires less power at the expense of extra bandwidth requirement (for a given bit rate). The bandwidth is directly proportional to the number of chips in a symbol interval whereas the power is inversely proportional to it. Due to its decreased power requirement, PPM is a suitable choice for portable infrared transmitters [4]. Another advantage of the PPM over PAM is that the near DC noise from fluorescent lamps has less effects on PPM [4].

In $M$-ary transmission with no strict bandwidth limitation, Gagliardi and Karp [59] have shown that the optimal modulation scheme in maximum likelihood sense for high background illumination consists of $M$ disjoint narrow pulses.

**Differential PPM (DPPM)**

To improve the spectral efficiency of PPM, differential PPM (DPPM) is designed [20, 60]. Another advantage of DPPM is that it only requires synchronization to the individual chips and not the symbol interval. In DPPM, the data is transmitted by omitting the zero chips following a pulse, so symbol duration is unequal. The DPPM requires less bandwidth and slightly more power than PPM.

Other variations of the PPM which increase its spectral efficiency while descreasing average optical power include: multiple PPM, overlapping PPM, pulse interval modulation and edge position modulation [4, 22, 31, 32, 55].

## 2.3.4 $M$-ary Quadrature Amplitude Modulation ($M$-QAM)

This is a two dimensional modulation format in which the data is sent over in-phase and quadrature dimensions of the channel. The bandwidth required for QAM is more than PAM (if we are not using subcarrier modulation). However, the power efficiency of QAM is more [22]. The reason is that QAM is two orthogonal PAM, and for the same average optical power, the distance between constellation points is more in QAM compared to PAM.

The QAM requires coherent transmission so the orthogonality between the in-phase and quadrature dimensions is maintained. As a result, we cannot utilize QAM in our application.

**Adaptively Biased QAM (AB-QAM)**

AB-QAM is a variation of QAM in which the DC bias changes in each symbol period according to the transmitted symbol in that interval [24] in a way that the transmitted signal in that period has minimum value equal to zero. As a result, power consumption for DC bias reduces. Another advantage of AB-QAM is that the DC bias (the third dimension) provides a degree of signal space diversity in the receiver and increases the minimum distance between symbols.

## 2.3.5 Optical Impulse Modulation

In this scheme [61], the information will be transmitted in lowpass frequencies. The high-pass frequencies which are attenuated by the channel contain no information, and are used to satisfy the amplitude constraint. As a result, they are suitable for bandlimited channels.

# 3  System Model

In this section, we consider the IM/DD transmission system with a strict bandwidth limitation and general $M$-level modulation. Fig. 3.1 represents the system model for an IM/DD optical transmission system. It can be modeled as an electrical baseband transmission system with AWGN and a nonnegativity constraint on the channel input [3, 4, 9, 62].

## 3.1  Transmitter

We consider an ergodic source with independent and identically distributed information symbols $a_k \in \mathcal{C}$, where $k \in \mathbb{Z}$ is the discrete time instant, and $\mathcal{C}$ is a finite set of constellation points. Based on these symbols, an electrical signal $I(t)$ is generated. The optical intensity modulator converts the electrical signal to an optical signal with optical carrier frequency $f_c$ and random phase $\theta$, given by

$$O(t) = \sqrt{2x(t)} cos\left(2\pi f_c t + \theta\right),$$

where $x(t)$ is the intensity of the optical signal. Information is transmitted by varying or modulating the optical intensity, in response to the driving electrical current signal, $I(t)$. As a result, this intensity is a linear function of $I(t)$ [4], given by

$$x(t) = JI(t) = JA\left(\mu + \sum_{k=-\infty}^{\infty} a_k q(t - kT_s)\right), \tag{3.1}$$

where $J$ is the laser conversion factor, $A$ is a scaling factor that can be adjusted depending on the desired transmitted power, $\mu$ is the required DC bias, $q(t)$ is an arbitrary pulse, and $T_s$ is the symbol duration.

Three requirements are placed on $x(t)$: it should be nonnegative, bandlimited, and
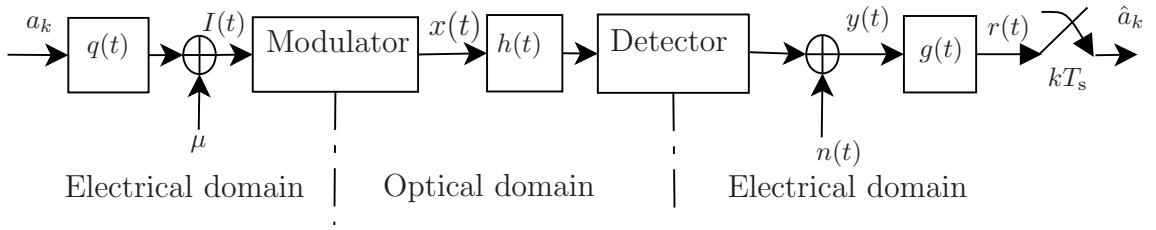
Figure 3.1. Baseband system model, where $a_k$ is the $k$-th input symbol, $q(t)$ is an arbitrary pulse, $\mu$ is the DC bias, $I(t)$ is the transmitted electrical signal, $x(t)$ is the optical intensity, $h(t)$ is the channel impulse response, $n(t)$ is the Gaussian noise, $g(t)$ is the impulse response of the receiver filter, and $\hat{a}_k$ is an estimate of $a_k$.

ISI-free. The nonnegativity constraint, $x(t) \geq 0$ for all $t \in \mathbb{R}$, is fulfilled by choosing $\mu$ in (3.1) sufficiently large, see Sec. 5. This DC bias is added equally to each symbol to maintain a strictly bandlimited signal $x(t)$, in contrast to works like [24, 34, 35] in which the bias is allowed to vary with time. The bandwidth constraint is fulfilled by choosing the pulse $q(t)$ such that

$$Q(\omega) = \int_{-\infty}^{\infty} q(t)e^{-j\omega t}dt = 0, \ |\omega| \geq 2\pi B, \tag{3.2}$$

where $Q(\omega)$ denotes the Fourier transform of $q(t)$. The condition of ISI-free transmission, finally, is fulfilled by either choosing $q(t)$ as a Nyquist pulse, see Sec. 4.2, when using a sampling receiver, or choosing $q(t)$ as a root-Nyquist pulse (also known as $T_{\mathrm{s}}$-orthogonal pulse), see Sec. 4.3, when using a matched filter in the receiver. Fig. 4.1 illustrates an example of the transmitted intensity given by (3.1) where $\mathcal{C} = \{0, 1\}$.

Depending on the application, it is desirable to minimize the average optical power or the peak optical power [4, 7–9, 26, 27]. The average optical power is

$$P_{\mathrm{opt}} = \frac{1}{T_{\mathrm{s}}} \int_{0}^{T_{\mathrm{s}}} \mathbb{E}\left\{x(t)\right\} dt,$$

where $\mathbb{E}\left\{\cdot\right\}$ denotes expectation, which for the definition of $x(t)$ in (3.1) yields

$$
\begin{aligned}
P_{\text{opt}} &= \frac{1}{T_{\text{s}}} \int_0^{T_{\text{s}}} JA\left(\mu + \mathbb{E}\left\{a_k\right\} \sum_{k=-\infty}^{\infty} q(t - kT_{\text{s}})\right) dt \\
&= JA\left(\mu + \mathbb{E}\left\{a_k\right\} \overline{q}\right),
\end{aligned}
\tag{3.3}
$$

where

$$
\overline{q} = \frac{1}{T_{\text{s}}} \int_{-\infty}^{\infty} q(t)dt = \frac{Q(0)}{T_{\text{s}}}.
\tag{3.4}
$$

The peak optical power is

$$
P_{\text{max}} = \max x(t) = JA\left(\mu + \max \sum_{k=-\infty}^{\infty} a_k q(t - kT_{\text{s}})\right)
\tag{3.5}
$$

where the maximum is taken over all symbol sequences $\ldots, a_{-1}, a_0, a_1, a_2, \ldots$ and all times $t$.

## 3.2   Channel

The described system can be modeled as a conventional linear channel with additive, white, signal independent, Gaussian noise [4] and nonnegative input [22, Ch. 5] [4, 26, 27, 63]. The analysis in this study covers two types of channels: (i) diffuse indoor wireless optical intensity channels, and (ii) short-haul fiber optic channels.

### 3.2.1   Diffuse Indoor Wireless Optical Intensity Channels

In case of diffuse indoor wireless optical intensity channels [3], the transmitted optical signal is radiated to the environment, and is detected by a photodetector. These channels are attractive for the following reasons: (i) Low-cost devices are used in this type of transmission. (ii) LED and photodiodes have compact size in contrast

to radio-frequency antennae. (iii) Since the photodiode receives the incoming signal from a wide field of view, there is no need for direct line of sight between transmitter and receiver [3]. (iv) The frequency range used in this type of transmission is not regulated [4]. (v) The detected signal is not affected by multipath fading since the photodiode benefits from spatial diversity by integrating the optical intensity field over an area of millions of square wavelengths [4, 62]. (vi) Since the radiations are in the infrared frequency range, they cannot pass through the wall or other opaque barriers. As a result, interference between the rooms do not happen [3, 22].

One drawback of this system is that since the receiver will detect the reflections of the signal off the surfaces, multipath distortion arises. As a result, the received signal in high-speed links suffers from severe ISI and limited bandiwdth [4, 5].

The intense ambient light in indoor environments (e.g., daylight, tungsten, and fluorescent lamps) is the main noise source in diffuse indoor wireless systems. The reason is that the photodiode produces shot noise if it is exposed to the ambient light. Assuming that the quantum fluctuations of the channel are negligible [4], the shot noise induced by the ambient light can be modeled as Gaussian since the noise consists of the superposition of many independent sources. In case of high-density shot noise, this approximation is highly accurate [63].

## 3.2.2   Short-haul Fiber Optic Channels

The invention of multimode fibers opened the door to the short-haul high-speed optical transmission systems [64]. Since they are inexpensive, they are used extensively in local area networks (LAN), fiber to the home (FTTH), and computer interconnects (connecting computers and chips within computers) [10]. The dominant noise source in these type of channels is the thermal noise caused by the electronic preamplifier.

The hardware bandwidth, chromatic and modal dispersions limit the transmission bandwidth over multimode fibers. Modal dispersion is the dominant impairment in short range applications, which puts a constraint on bandwidth×distance (modal bandwidth expressed in MHz.km). As a result, multimode fibers are used for optical interconnects which are around a few hundred meters [10]. In FTTH with length around 5-10 km, single-mode fibers are used which have a bandwidth constraint approximately equal to 40 GHz [65].

Another reason for bandwidth constraint which is common for both type of channels is reverse bias depletion capacitances which is generated due to the implementation of inexpensive, large area photodiodes in the receivers [5].

## 3.3   Receiver

In the receiver, the direct-detection method is used in which the photodetector generates an output electrical current which is proportional to the incident received instantaneous optical power [24]. To do so, electron-hole pairs are generated in the depletion layer of the device by the incident photons. These carriers are swept out by the large electric field in the region [24]. The optical signal then propagates through the channel and is detected and converted to the electrical signal [4, 26]

$$y(t) = Rh(t) \otimes x(t) + n(t),$$

where $R$ is the responsivity of the photodetector which represents an optoelectrical conversion factor (from optical intensity signal to electrical current signal), $\otimes$ is the convolution operator, $h(t)$ is the channel impulse response, and $n(t)$ is the noise. In this study, the channel is considered to be flat in the bandwidth of interest, i.e., $h(t) = H(0)\delta(t)$. Without loss of generality, we assume that $R = J = 1$ [4] and $H(0) = 1$. Since the thermal noise of the receiver and the shot noise induced by

ambient light are two major noise sources in this setup, which are independent from the signal, $n(t)$ can be modeled as a zero-mean AWGN with double-sided power spectral density $N_0/2$ [4, 6, 27, 37]. Although the input signal to the channel $x(t)$ must be nonnegative, there is no such constraint on the received signal $y(t)$ [25].

The received signal passes through a filter with impulse response $g(t)$, resulting in

$$r(t) = y(t) \otimes g(t), \tag{3.6}$$

which is then sampled at the symbol rate. From these samples, the received symbol will be estimated. In this study, two scenarios are considered for the receiver filter:

(i) Similarly to [9, 50], $y(t)$ can enter a sampling receiver, which in this study is assumed to have a rectangular frequency response to limit the power of the noise in the receiver, and is given by

$$G(\omega) = \begin{cases} G(0) & |\omega| < 2\pi B \\ 0 & |\omega| \geq 2\pi B \end{cases}. \tag{3.7}$$

(ii) According to our proposed method, $y(t)$ can enter a matched filter receiver with frequency response

$$G(\omega) = \zeta Q^*(\omega)$$

where $(\cdot)^*$ is the complex conjugate and $\zeta$ is an arbitrary scaling factor. This type of filter will limit the power of the noise, and can also result in ISI-free transmission if the pulses are root-Nyquist (see Sec. 4.3).

The system model introduced in this section is a generalization of the one in [9], which is obtained by considering $\mathcal{C} \subset \mathbb{R}^+$ and setting $\mu = 0$ in (3.1). If $\mu = 0$, the pulse $q(t)$ should be nonnegative to guarantee a nonnegative signal $x(t)$. In our

proposed system model, by introducing the bias $\mu$, the nonnegativity condition can be fulfilled for a wider selection of pulses $q(t)$ and constellation $\mathcal{C} \subset \mathbb{R}$.

# 4 AN OVERVIEW OF PULSES

## 4.1 The Criteria in Selecting the Pulse

In order to have ISI-free transmission with a sampling receiver, the transmitted pulse $q(t)$ defined in Sec. 3.1 must satisfy the Nyquist criterion [11]. In other words, for any $k \in \mathbb{Z}$ [6, Eq. (9.2-11)],

$$
q(kT_{\mathrm{s}}) = \begin{cases} q(0) & k = 0 \\ 0 & k \neq 0 \end{cases}.
\tag{4.1}
$$

In frequency domain, the Nyquist criterion can be written as

$$
\frac{1}{T_{\mathrm{s}}} \sum_{k=-\infty}^{\infty} Q(\omega - \frac{k2\pi}{T_{\mathrm{s}}}) = q(0).
\tag{4.2}
$$

This criterion guarantees that a sequence of pulses sampled at the optimum, uniformly spaced sampling instants, $k = ..., -2, -1, 0, 1, 2, ...$, will have zero ISI.

## 4.2 Nyquist Pulses

The pulses that satisfy condition (4.1) are called Nyquist pulses. In some references, these pulses are called Nyquist-I pulses, since there are three criteria defined by Nyquist and condition (4.1) is the first criterion.

The most popular Nyquist pulses are the classical "sinc" pulse, defined as $\mathrm{sinc}(x) = \sin(\pi x)/(\pi x)$, and the raised-cosine (RC) pulse [6, Sec. 9.2]. Many other Nyquist pulses have been proposed recently for the conventional channel; see [66, 67] and references therein.

## 4.2.1   Regular Nyquist Pulses

In this section, we consider four Nyquist pulses that have been studied for the conventional coherent channel. In all cases, the bandwidth can be adjusted via the roll-off factor $\alpha$ chosen in the range $0 \leq \alpha \leq 1$. Since these pulses can be negative, they must be used in a system with $\mu > 0$. We denote these four pulses as *regular* Nyquist pulses.

(i) Raised-cosine (RC) pulse which is one of the most popular Nyquist pulses and is defined as

$$q_{\mathrm{RC}}(t) = \mathrm{sinc}\left(\frac{t}{T_{\mathrm{s}}}\right)\left(\frac{\cos(\alpha\pi t/T_{\mathrm{s}})}{1 - (\frac{2\alpha t}{T_{\mathrm{s}}})^2}\right). \tag{4.3}$$

The tails of this pulse decay asymptotically as $t^{-3}$. The RC pulse is a low-pass filter with odd symmetry around a cutoff frequency and has a cosine shaped roll-off portion [11].

(ii) The parametric linear (PL) pulse of first order defined in [13], which is given by [68]

$$q_{\mathrm{PL}}(t) = \mathrm{sinc}\left(\frac{t}{T_{\mathrm{s}}}\right)\mathrm{sinc}\left(\alpha\frac{t}{T_{\mathrm{s}}}\right). \tag{4.4}$$

and decays as $1/t^2$. The advantage of this pulse compared to RC pulse is its less sensitivity to timing jitter.

(iii) The so-called "better than Nyquist" (BTN) pulse [16], which in [13] was referred to as parametric exponential pulse, given by

$$q_{\mathrm{BTN}}(t) = \mathrm{sinc}\left(\frac{t}{T_{\mathrm{s}}}\right)\frac{4\beta\pi t\sin\left(\frac{\pi\alpha t}{T_{\mathrm{s}}}\right) + 2\beta^2\cos\left(\frac{\pi\alpha t}{T_{\mathrm{s}}}\right) - \beta^2}{4\pi^2 t^2 + \beta^2}, \tag{4.5}$$

where $\beta = 2T_{\mathrm{s}}\ln 2/\alpha$. The tails of this pulse decay as $t^{-2}$. The magnitudes of the two largest sidelobes of the RC pulse are larger than the magnitudes of the two largest sidelobes of the BTN or PL. The maximum distortion (the magnitude of the

largest possible ISI sample at any given time instant) , which occurs at $t/T_s = 0.5$, is less for the BTN and PL than the RC pulse.

(iv) The polynomial (Poly) pulse designed in [18] which has fast asymptotic decay rate (ADR) and flexible design even after the $\alpha$ is selected. This pulse for ADR of $t^{-4}$ is defined as

$$
q(t) = \begin{cases} 1, & t = 0, \\ 3\,\text{sinc}\left(\frac{t}{T_s}\right) \dfrac{\text{sinc}\left(\frac{\alpha t}{2T_s}\right)^2 - \text{sinc}\left(\frac{\alpha t}{T_s}\right)}{\left(\frac{\pi \alpha t}{2T_s}\right)^2}, & \text{otherwise} \end{cases}
$$

All these pulses have a lowpass bandwidth $B = (1 + \alpha)/(2T_s)$ and $\overline{q} = 1$.

## 4.2.2   Nonnegative Nyquist Pulses

In this section, which is motivated by [9], all the three aforementioned constraints (see Section 3.1) should be satisfied by the pulse. As a result, in (3.1), $\mu = 0$ and $q(t) \geq 0$ for all $t \in \mathbb{R}$. As in Sec. 4.2.1, the roll-off factor $\alpha$ satisfies $0 \leq \alpha \leq 1$.

In [9], it has been shown that pulses that satisfy these three requirements must be the square of a general Nyquist pulse. This will result in having pulses with bandwidth twice that of the original Nyquist pulses. Three pulses that satisfy these constraints were introduced in [9], and we use them in our study for compatibility with previous works:

(i) Squared sinc (S2), which is given by

$$
q_{S2}(t) = \text{sinc}^2 \left( \frac{t}{T_s} \right), \tag{4.6}
$$

has the lowpass bandwidth $B = 1/T_s$ and $\overline{q} = 1$.

(ii) Squared RC (SRC), given by

$$q_{\text{SRC}}(t) = q_{\text{RC}}^2(t), \tag{4.7}$$

requires a larger lowpass bandwidth $B = (1 + \alpha)/T_\text{s}$ compared to S2, and $\overline{q} = 1 - \frac{\alpha}{4}$.

(iii) Squared double-jump (SDJ), given by

$$q_{\text{SDJ}}(t) = \left[ \left( \frac{1 - \alpha}{2} \right) \text{sinc} \left( \frac{(1 - \alpha)t}{T_\text{s}} \right) + \left( \frac{1 + \alpha}{2} \right) \text{sinc} \left( \frac{(1 + \alpha)t}{T_\text{s}} \right) \right]^2, \tag{4.8}$$

requires the same lowpass bandwidth as SRC (i.e., $B = (1 + \alpha)/T_\text{s}$), but has a lower $\overline{q}$ for a given $\alpha$ than the other two pulses, $\overline{q} = 1 - \frac{\alpha}{2}$.

Double-jump (DJ) pulses [12] were designed to minimize the mean-square error due to time-jitter for a specified value of $\alpha$. This pulse is called double-jump since in frequency domain it possesses two jump discontinuities at $f = (1 - \alpha)/(2T_\text{s})$ and $f = (1 + \alpha)/(2T_\text{s})$ [69](see [12, Fig. 2]).

Figs. 4.1 and 4.2 depict the normalized transmitted signal $x(t)/A$ using the RC (4.3) and SRC (4.7) pulses, respectively assuming $\mathcal{C} = \{0, 1\}$. The most important parameters of the pulses are summarized in Table 4.1.

## 4.3   Bandlimited Root-Nyquist Pulses

ISI-free transmission is achieved with the pulses in Sec. 4.2 as long as the input of the sampling unit satisfies the Nyquist criterion given in (4.1). In addition to the method of using a Nyquist pulse in the transmitter and a rectangular filter (3.7) in the receiver, other scenarios can be designed that generate Nyquist pulses at the input $r(t)$ of the sampling unit. In one of these methods, the transmitted pulse is a root-Nyquist pulse, and the receiver contains a filter matched to the transmitted pulse [6, Sec. 5.1] [70–72]. Consequently, the output of the matched filter will be ISI-free if for any integer $k$

Figure 4.1.   The normalized transmitted signal $x(t)/A$ for $\mathcal{C} = \{0, 1\}$ and using an RC pulse (4.3) with $\alpha = 0.6$ as $q(t)$. It can be seen that without using the bias $\mu = 0.184$, the RC pulse would create a signal $x(t)$ that can be negative.
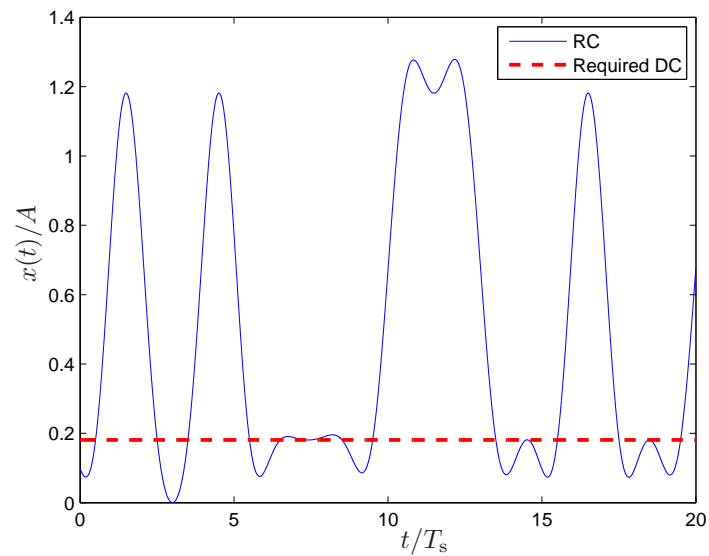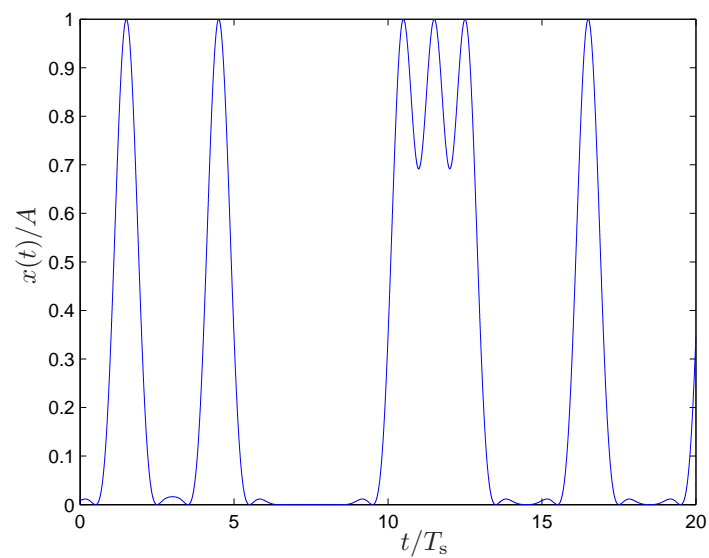


Figure 4.2.   The normalized transmitted signal $x(t)/A$ for $\mathcal{C} = \{0, 1\}$ and using an SRC pulse (4.7) with $\alpha = 0.6$ as $q(t)$. In this case, the required DC $\mu$ is zero.

Table 4.1.   Parameters of all considered pulses.  The energy $E_q$ is relevant for root-Nyquist pulses only.

| Pulse | Nyquist | root-Nyquist | $\overline{q}$ | $q(0)$ | $BT_\mathrm{s}$ | $E_q/T_\mathrm{s}$ |
|:-----:|:-------:|:------------:|:--------------:|:------:|:---------------:|:------------------:|
| RC    | ✓ |   | 1 | 1 | $(1+\alpha)/2$ | |
| BTN   | ✓ |   | 1 | 1 | $(1+\alpha)/2$ | |
| PL    | ✓ |   | 1 | 1 | $(1+\alpha)/2$ | |
| Poly  | ✓ |   | 1 | 1 | $(1+\alpha)/2$ | |
| S2    | ✓ |   | 1 | 1 | $1$ | |
| SRC   | ✓ |   | $1-\alpha/4$ | 1 | $1+\alpha$ | |
| SDJ   | ✓ |   | $1-\alpha/2$ | 1 | $1+\alpha$ | |
| RRC   |   | ✓ | 1 | $1-\alpha+4\alpha/\pi$ | $(1+\alpha)/2$ | 1 |
| Xia   | ✓ | ✓ | 1 | 1 | $(1+\alpha)/2$ | 1 |

$$\int\limits_{-\infty}^{\infty} q(t)q(t - kT_\mathrm{s})dt = \begin{cases} E_q & k = 0 \\ 0 & k \neq 0 \end{cases}, \tag{4.9}$$

where $E_q = \int_{-\infty}^{\infty} q^2(t)dt$.

In designing transmit and receive filters for data transmission, having zero ISI, a linear phase characteristic, being matched to the transmitter filter, and small bandwidth are main issues [73]. Furthermore, since for the digital implementation of the filters, they are truncated, the output of the matched filter receiver in practice is not Nyquist anymore. This is the reason that those root-Nyquist pulses with tails that decay rapidly are preferable to reduce the resulting ISI.

Table 4.1 also includes two root-Nyquist pulses that have been previously used for conventional coherent channels, where again $0 \leq \alpha \leq 1$: (i) Root-RC (RRC) pulse, which is given by (4.10)

$$q_{\mathrm{RRC}}(t) = \begin{cases} 1 - \alpha + \frac{4\alpha}{\pi} & t = 0 \\ \frac{\alpha}{\sqrt{2}}\left[(1 + \frac{2}{\pi})sin(\frac{\pi}{4\alpha}) + (1 - \frac{2}{\pi})cos(\frac{\pi}{4\alpha})\right] & t = \pm\frac{T_\mathrm{s}}{4\alpha} \\ \frac{sin\left(\pi\frac{t}{T_\mathrm{s}}(1-\alpha)\right) + 4\alpha\frac{t}{T_\mathrm{s}}cos\left(\pi\frac{t}{T_\mathrm{s}}(1+\alpha)\right)}{\pi\frac{t}{T_\mathrm{s}}\left(1 - \left(4\alpha\frac{t}{T_\mathrm{s}}\right)^2\right)} & \text{otherwise} \end{cases} \tag{4.10}$$

(ii) First order Xia pulse [74], which is given by

$$q_{\text{Xia}}(t) = \text{sinc}\left(\frac{t}{T_{\text{s}}}\right) \frac{\cos\left(\frac{\alpha\pi t}{T_{\text{s}}}\right)}{\left(2\alpha\left(\frac{t}{T_{\text{s}}}\right) + 1\right)}. \tag{4.11}$$

Both RRC and Xia pulses have the lowpass bandwidth $B = (1 + \alpha)/(2T_{\text{s}})$, and $\overline{q} = 1$.

The Xia pulse is an example of the conjugate-root pulses used to have ISI-free transmission. In this case, the complex conjugate roots of the frequency response of a Nyquist pulse (RC pulse for (4.11)) is used to derive the pulse [74–77]. The conjugate-root pulses do not have better performance compared to matched filter receivers [78]. Their main application is when the matched filter is used solely to eliminate ISI. So the complexity can be reduced by using a pulse which satisfies Nyquist criterion alone or with matched filter.

Although the output of the matched filter for both the first order Xia pulse and the RRC pulse are similar ($r(t)$ consists of RC pulses in both cases), the RRC is symmetric in time, whereas the Xia pulse has more energy in the precursor (i.e., the part of the pulse before the peak) [78]. This is visible in part (d) of Fig. 6.1. Moreover, the maximum of a Xia pulse does not happen at the origin. The important point with the Xia pulse is that it is both a Nyquist and a root-Nyquist pulse.

In contrast to the general Nyquist pulses from which nonnegative Nyquist pulses can be generated by squaring the original Nyquist pulse (see Sec. 4.2.2), the square of a root-Nyquist pulse is not root-Nyquist anymore. Moreover, [9] has proven that there is no nonnegative root-Nyquist pulse with strictly limited bandwidth.

A summary of all the pulses used in this report is provided in Table 4.2.

Table 4.2. Definitions of the studied Nyquist and root-Nyquist pulses.

| Pulse | Definition $q(t)$ |
|---|---|
| RC | $\begin{cases} \frac{\pi}{4}\operatorname{sinc}\left(\frac{t}{T_{\mathrm{s}}}\right), & t=\pm\frac{T_{\mathrm{s}}}{2\alpha}, \\ \operatorname{sinc}\left(\frac{t}{T_{\mathrm{s}}}\right)\frac{\cos\left(\frac{\pi\alpha t}{T_{\mathrm{s}}}\right)}{1-\left(\frac{2\alpha t}{T_{\mathrm{s}}}\right)^2}, & \text{otherwise} \end{cases}$ |
| BTN | $\operatorname{sinc}\left(\frac{t}{T_{\mathrm{s}}}\right)\dfrac{\frac{2\pi\alpha t}{T_{\mathrm{s}}\ln 2}\sin\left(\frac{\pi\alpha t}{T_{\mathrm{s}}}\right)+2\cos\left(\frac{\pi\alpha t}{T_{\mathrm{s}}}\right)-1}{\left(\frac{\pi\alpha t}{T_{\mathrm{s}}\ln 2}\right)^2+1}$ |
| PL | $\operatorname{sinc}\left(\frac{t}{T_{\mathrm{s}}}\right)\operatorname{sinc}\left(\frac{\alpha t}{T_{\mathrm{s}}}\right)$ |
| Poly | $\begin{cases} 1, & t=0, \\ 3\operatorname{sinc}\left(\frac{t}{T_{\mathrm{s}}}\right)\dfrac{\operatorname{sinc}\left(\frac{\alpha t}{2T_{\mathrm{s}}}\right)^2-\operatorname{sinc}\left(\frac{\alpha t}{T_{\mathrm{s}}}\right)}{\left(\frac{\pi\alpha t}{2T_{\mathrm{s}}}\right)^2}, & \text{otherwise} \end{cases}$ |
| S2 | $\operatorname{sinc}^2\left(\frac{t}{T_{\mathrm{s}}}\right)$ |
| SRC | $q_{\mathrm{RC}}^2(t)$, where $q_{\mathrm{RC}}$ is the RC pulse defined above |
| SDJ | $\left[\left(\frac{1-\alpha}{2}\right)\operatorname{sinc}\left(\frac{(1-\alpha)t}{T_{\mathrm{s}}}\right)+\left(\frac{1+\alpha}{2}\right)\operatorname{sinc}\left(\frac{(1+\alpha)t}{T_{\mathrm{s}}}\right)\right]^2$ |
| RRC | $\begin{cases} 1-\alpha+\frac{4\alpha}{\pi}, & t=0, \\ \frac{\alpha}{\sqrt{2}}\left[\left(1+\frac{2}{\pi}\right)\sin(\frac{\pi}{4\alpha})+\left(1-\frac{2}{\pi}\right)\cos(\frac{\pi}{4\alpha})\right], & t=\pm\frac{T_{\mathrm{s}}}{4\alpha}, \\ \dfrac{\sin\left(\frac{\pi(1-\alpha)t}{T_{\mathrm{s}}}\right)+\frac{4\alpha t}{T_{\mathrm{s}}}\cos\left(\frac{\pi(1+\alpha)t}{T_{\mathrm{s}}}\right)}{\frac{\pi t}{T_{\mathrm{s}}}\left(1-\left(\frac{4\alpha t}{T_{\mathrm{s}}}\right)^2\right)}, & \text{otherwise} \end{cases}$ |
| Xia | $\operatorname{sinc}\left(\frac{t}{T_{\mathrm{s}}}\right)\dfrac{\cos\left(\frac{\pi\alpha t}{T_{\mathrm{s}}}\right)}{\frac{2\alpha t}{T_{\mathrm{s}}}+1}$ |

# 4.4   Other Pulses

Hranilovic [9] has proved that the nonnegative root-Nyquist pulses must be time limited. Moreover, he has investigated the family of prolate spheroidal wave functions which consists of time limited pulses that have the lowest bandwidth among functions limited to $[-T_{\mathrm{s}}/2, T_{\mathrm{s}}/2]$ [52]. It was mentioned that the zeroth member of this family is both a smooth function of time and has no zero crossings in $[T_{\mathrm{s}}/2, T_{\mathrm{s}}/2]$ [79]. As a result, it is nonnegative pulse with approximately limited bandwidth.

# 5  THE REQUIRED DC BIAS

Our goal is to find the lowest $\mu$ that guarantees the nonnegativity of $x(t)$. From (3.1) and $x(t) \geq 0$, the smallest required DC bias is

$$\mu = - \min_{\forall a, -\infty < t < \infty} \sum_{k=-\infty}^{\infty} a_k q(t - kT_s) \tag{5.1}$$

$$= - \min_{\forall a, -\infty < t < \infty} \sum_{k=-\infty}^{\infty} \left[ (a_k - L) \, q(t - kT_s) + Lq(t - kT_s) \right] \tag{5.2}$$

where $L = (\hat{a} + \check{a})/2$, $\hat{a} = \max_{a \in \mathcal{C}} a$, and $\check{a} = \min_{a \in \mathcal{C}} a$. The notation $\forall a$ in (5.1) and (5.2) means that the minimization should be over all $a_k \in \mathcal{C}$ where $k = \dots, -1, 0, 1, 2, \dots$ Going from (5.1) to (5.2), we created a factor $(a_k - L)$ which is a function of $a_k$ and symmetric with respect to zero. As a result, the minimum of the first term in (5.2) occurs if, for all $k$, either $a_k = \hat{a}$ and $q(t - kT_s) < 0$ or $a_k = \check{a}$ and $q(t - kT_s) > 0$. In both cases, due to the fact that the factor $\hat{a} - L = -(\check{a} - L)$,

$$\mu = \max_{0 \leq t < T_s} \left[ (\hat{a} - L) \sum_{k=-\infty}^{\infty} |q(t - kT_s)| - L \sum_{k=-\infty}^{\infty} q(t - kT_s) \right]. \tag{5.3}$$

The reason why (5.3) is minimized over $0 \leq t < T_s$ is that $\sum_{i=-\infty}^{\infty} q(t - iT_s)$ and $\sum_{i=-\infty}^{\infty} |q(t - iT_s)|$ are periodic functions with period equal to $T_s$. Since for all pulses defined in Sec. 4.2 and 4.3, $q(t)$ rescales with $T_s$ as $q(t) = v(t/T_s)$ for some function $v(t)$, then $\mu$ is independent of $T_s$.

To simplify (5.3), Lemma 1 and Corollary 2 will be helpful, since they prove that the second term in (5.3) does not change over time.

**Lemma 1.** *For an arbitrary pulse $q(t)$,*

$$\sum_{k=-\infty}^{\infty} q(t - kT_\mathrm{s}) = \frac{1}{T_\mathrm{s}} \sum_{n=-\infty}^{\infty} Q\left(\frac{2\pi n}{T_\mathrm{s}}\right) e^{\frac{j2\pi nt}{T_\mathrm{s}}}.$$

*Proof.* Since $f(t) = \sum_{k=-\infty}^{\infty} q(t - kT_\mathrm{s})$ is a periodic function with period $T_\mathrm{s}$, it can be expanded as a Fourier series. Its Fourier series coefficients are

$$
\begin{aligned}
C_n &= \frac{1}{T_\mathrm{s}} \int\limits_{-T_\mathrm{s}/2}^{T_\mathrm{s}/2} f(t) e^{-\frac{j2\pi nt}{T_\mathrm{s}}} dt \\
&= \frac{1}{T_\mathrm{s}} \int\limits_{-T_\mathrm{s}/2}^{T_\mathrm{s}/2} \sum_{k=-\infty}^{\infty} q(t - kT_\mathrm{s}) e^{-\frac{j2\pi nt}{T_\mathrm{s}}} dt.
\end{aligned}
\tag{5.4}
$$

Since both $n$ and $k$ are integers, $e^{j2\pi nk} = 1$. As a result, (5.4) can be written as

$$
\begin{aligned}
C_n &= \frac{1}{T_\mathrm{s}} \int\limits_{-T_\mathrm{s}/2}^{T_\mathrm{s}/2} \sum_{k=-\infty}^{\infty} q(t - kT_\mathrm{s}) e^{-\frac{j2\pi n}{T_\mathrm{s}}(t - kT_\mathrm{s})} dt \\
&= \frac{1}{T_\mathrm{s}} \int\limits_{-\infty}^{\infty} q(t) e^{-\frac{j2\pi nt}{T_\mathrm{s}}} dt = \frac{1}{T_\mathrm{s}} Q\left(\frac{2\pi n}{T_\mathrm{s}}\right).
\end{aligned}
$$

Hence,

$$f(t) = \sum_{n=-\infty}^{\infty} C_n e^{\frac{j2\pi nt}{T_\mathrm{s}}} = \frac{1}{T_\mathrm{s}} \sum_{n=-\infty}^{\infty} Q\left(\frac{2\pi n}{T_\mathrm{s}}\right) e^{\frac{j2\pi nt}{T_\mathrm{s}}}, \tag{5.5}$$

which proves the lemma.                                                                            $\square$

The usefulness of this lemma follows from the fact that for bandlimited pulses $q(t)$, (5.5) is reduced to a finite number of terms. As a special case, we have the following corollary.

**Corollary 2.** *If $q(t)$ is a bandlimited pulse defined in (3.2), where $BT_\mathrm{s} \leq 1$, then (5.5) can be written as*

$$f(t) = \sum_{k=-\infty}^{\infty} q(t - kT_{\mathrm{s}}) = \frac{1}{T_{\mathrm{s}}} Q(0). \tag{5.6}$$

*In other words, for such q(t), this sum is not a function of time.*

*Proof.* Since $BT_{\mathrm{s}} \leq 1$, the sum in (5.5) has only one nonzero term (i.e., $Q(0)$ can be nonzero whereas $Q(2\pi n/T_{\mathrm{s}}) = 0$ for all $n \neq 0$ due to (3.2)). $\qquad \square$

As a result of Corollary 2, (5.3) for the regular Nyquist pulses and root-Nyquist pulses considered in Sec. 4.2.1 and Sec. 4.3 (but not SRC and SDJ) can be written as

$$\mu = (\hat{a} - L) \max_{0 \leq t < T_{\mathrm{s}}} \left[ \sum_{i=-\infty}^{\infty} |q(t - iT_{\mathrm{s}})| \right] - L \frac{Q(0)}{T_{\mathrm{s}}}, \tag{5.7}$$

where $Q(0) = \overline{q} T_{\mathrm{s}}$ for all pulses, see (3.4). It appears that solving the summation in (5.7) is impossible analytically even for simple pulses.

**Theorem 3.** *For bandlimited pulses where $BT_{\mathrm{s}} \leq 1$, the transmitted signal (3.1) is unchanged if all constellation points in $\mathcal{C}$ are shifted by a constant offset.*

*Proof.* Since the chosen pulse has limited bandwidth given by (3.2), using (5.6) given in Corollary 2, the transmitted signal (3.1) can be written as

$$x(t) = A \left( \mu + \sum_{k=-\infty}^{\infty} (a_k - L + L) \, q\left(t - kT_{\mathrm{s}}\right) \right)$$

$$= A \left( \mu + \sum_{k=-\infty}^{\infty} (a_k - L) \, q\left(t - kT_{\mathrm{s}}\right) + L \frac{Q(0)}{T_{\mathrm{s}}} \right). \tag{5.8}$$

Substituting the required bias given by (5.7), (5.8) can be written as

$$x(t) = A \left( (\hat{a} - L) \max_{0 \leq t < T_{\mathrm{s}}} \left[ \sum_{i=-\infty}^{\infty} |q(t - iT_{\mathrm{s}})| \right] + \sum_{k=-\infty}^{\infty} (a_k - L) \, q\left(t - kT_{\mathrm{s}}\right) \right). \tag{5.9}$$

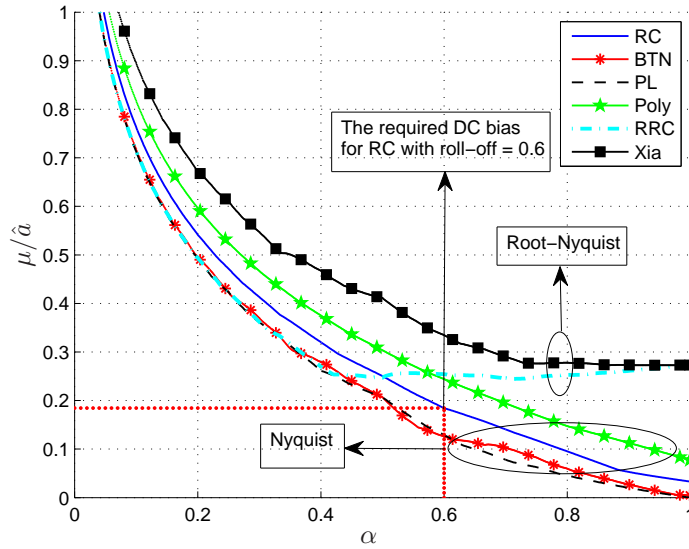It can be seen that (5.9) only depends on symbols through $\hat{a} - L$ and $a_k - L$. Both

Figure 5.1.    The normalized minimum DC bias $\mu/\hat{a}$ vs. roll-off factor $\alpha$ for a variety of pulses and $M$-PAM. The dotted line represents the required bias for the RC pulse at $\alpha = 0.6$, see Fig. 4.1.

terms are independent of the constellation offset.                                              □

Theorem 3 shows that for narrow-band pulses defined in (3.2), the constellation offset does not have an effect on the performance. This result which holds for intensity modulated channels (with nonnegative transmitted signal requirement) is in contrast to the standard result for conventional channels. For instance, binary phase-shift keying (BPSK) and OOK are equivalent in this IM/DD system, whereas BPSK is 3 dB better over the conventional AWGN channel [6, Sec. 5].

Fig. 5.1 illustrates the required DC bias (5.7) for various pulses considering any nonnegative $M$-PAM constellation ($\mathcal{C} = \{0, 1, ..., M - 1\}$). In case of Nyquist pulses, due to the fact that by increasing $\alpha$, the ripples of the pulses decrease, the required DC bias decreases as well. It can be seen that the Poly and RC pulses (4.3) always require more DC bias than other Nyquist pulses. Moreover, the PL (4.4) and the BTN (4.5) pulses require approximately the same DC bias. The BTN pulse requires slightly less DC bias in $0.250 \leq \alpha \leq 0.256$, $0.333 \leq \alpha \leq 0.363$, and $0.500 \leq \alpha \leq$

0.610, while the PL is better for all other roll-off factors in the range $0 < \alpha < 1$.

The RRC (4.10) has a different behavior. For $0 < \alpha \leq 0.420$, similar to Nyquist pulses, by increasing the roll-off factor, the required DC bias decreases, and is approximately equal to the required DC bias for BTN and PL. However, when $0.420 \leq \alpha < 1$, the required DC bias starts to fluctuate slightly around $\mu = 0.25\hat{a}$ and the minimum happens for $\alpha = 0.715$. The reason for this behavior is that in RRC, the peak is a function of $\alpha$, see (4.10). As a result, by increasing the roll-off factor, there will be a compromise between the reduction in the sidelobe amplitude and the increase in peak amplitude. For small values of $\alpha$, the sidelobe reduction is more significant than the peak increase, and as a result, the required DC bias decreases. The Xia pulse (4.11) always requires the largest DC bias. For $0 < \alpha \leq 0.730$, similar to other pulses, by increasing the roll-off factor, the required DC bias for Xia pulses decreases. However, when $0.730 \leq \alpha < 1$, the required DC bias starts to fluctuate slightly and starts to approach the required DC for RRC.

The expression for $\mu$ given in (5.3) illustrates the reason why the double-jump and sinc pulses are not considered in Sec. 4.2.1. These pulses decay as $1/|t|$. As a result, the summation in (5.3) does not converge to a finite value. Hence, they require an infinite amount of DC bias to be nonnegative.

# 6 ANALYSIS AND RESULTS

## 6.1 Received Sequence Analysis

### 6.1.1 Received Sequence for Sampling Receiver

Considering the assumptions mentioned in Sec. 3, the received signal (3.6) is

$$r(t) = (x(t) + n(t)) \otimes g(t) \tag{6.1}$$

$$= A \left( \mu + \sum_{k=-\infty}^{\infty} a_k q(t - kT_s) \right) \otimes g(t) + z(t) \tag{6.2}$$

$$= AG(0) \left[ \mu + \sum_{k=-\infty}^{\infty} a_k q(t - kT_s) \right] + z(t), \tag{6.3}$$

where (6.3) holds since $g(t)$ has a flat frequency response given by (3.7) over the bandwidth of $q(t)$ given by (3.2); Therefore, the convolution has no effect on $x(t)$. The noise at the output of the receiver filter, which is given by $z(t) = n(t) \otimes g(t)$, is zero mean additive white Gaussian with variance $\sigma_z^2 = G(0)^2 N_0 B$.

Applying the Nyquist criterion given in (4.1) to the sampled version of (6.3), we can write the $i$-th filtered sample as

$$r(iT_s) = AG(0) \left[ \mu + a_i q(0) \right] + z(iT_s). \tag{6.4}$$

for any constellation $\mathcal{C}$. The received waveform $r(t)$, for several Nyquist pulses, is shown in Fig. 6.1, in the form of eye diagrams in a noise-free setting ($z(t) = 0$). As expected, the output samples $r(iT_s)$ are ISI-free.

## 6.1.2 Received Sequence for Matched Filter Receiver

Similar to Sec. 6.1.1, the received signal will be

$$r(t) = (x(t) + n(t)) \otimes g(t)$$

$$= A \left( \mu + \sum_{k=-\infty}^{\infty} a_k q(t - kT_s) \right) \otimes \zeta q(-t) + u(t)$$

$$= A\zeta \left( \mu \int_{-\infty}^{\infty} q(-t)dt + \sum_{k=-\infty}^{\infty} a_k \int_{-\infty}^{\infty} q(\tau - kT_s)q(\tau - t)d\tau \right) + u(t)$$

$$= A\zeta \left( \mu Q(0) + \sum_{k=-\infty}^{\infty} a_k \int_{-\infty}^{\infty} q(\tau)q(\tau - t + kT_s)d\tau \right) + u(t) \qquad (6.5)$$

where $u(t)$ is zero mean additive white Gaussian noise with variance $\sigma_u^2 = \zeta^2 N_0 E_q / 2$. Applying the root-Nyquist criterion given in (4.9) to the sampled version of (6.5), the $i$-th filtered sample will be, for any constellation $\mathcal{C}$,

$$r(iT_s) = A\zeta \left( \mu Q(0) + a_i E_q \right) + u(iT_s). \qquad (6.6)$$

## 6.2 Comparison Between the Pulses

As mentioned in Sec. 3, it may be desirable to minimize the average or peak optical power. The next theorem shows that these two criteria are equivalent for narrow-band pulses $(BT_s < 1)$ and symmetric constellations $(\mathbb{E}\{a_k\} = L)$.

**Theorem 4.** *If $BT_s < 1$ and $\mathbb{E}\{a_k\} = L$, then $P_{\max} = 2P_{\text{opt}}$.*

*Proof.* From (3.5) and Corollary 2,

$$P_{\max} = JA \left( \mu + \max_{\forall a, -\infty < t < \infty} \sum_{k=-\infty}^{\infty} \left[ (a_k - L) q(t - kT_s) + Lq(t - kT_s) \right] \right)$$

$$= JA \left( \mu + \max_{\forall a, -\infty < t < \infty} \left[ \sum_{k=-\infty}^{\infty} (a_k - L) q(t - kT_s) + \frac{LQ(0)}{T_s} \right] \right).$$

In analogy to (5.7), the maximum is

$$P_{\max} = JA\left(\mu + (\hat{a} - L)\max_{0 \le t < T_s}\sum_{k=-\infty}^{\infty}|q(t - kT_s)| + \frac{LQ(0)}{T_s}\right) = JA\left(2\mu + 2\frac{LQ(0)}{T_s}\right)$$

which compared with (3.3) completes the proof.                                                              □

To compare the optical power of various pulses, a criterion called optical power gain is used, which is defined as [9]

$$\Upsilon = 10\log_{10}\left(\frac{P_{\text{opt}}^{\text{ref}}}{P_{\text{opt}}}\right),$$

where $P_{\text{opt}}^{\text{ref}}$ is the average optical power for a reference system (according to Theorem 4, $\Upsilon$ would be the same if defined in terms of $P_{\max}$, for all pulses in our study except SRC and SDJ). Similarly to [50], this reference is chosen to be the S2 pulse (4.6) with OOK modulation and sampling receiver, for which no bias is needed. Using (3.3), $P_{\text{opt}}^{\text{ref}} = A_{\text{ref}}\mathbb{E}_{\text{ref}}\{a_k\}$ and

$$\Upsilon = 10\log_{10}\left(\frac{A_{\text{ref}}\mathbb{E}_{\text{ref}}\{a_k\}}{A\left(\mu + \mathbb{E}\{a_k\}\,\overline{q}\right)}\right) \tag{6.7}$$

where $A_{\text{ref}}$ and $\mathbb{E}_{\text{ref}}\{a_k\}$ are the scaling factor and the symbol average for the reference system, resp. Defining

$$\Delta a = \min_{a,a' \in \mathcal{C}, a \ne a'}|a - a'| \tag{6.8}$$

as the minimum distance between any two constellation points $a$ and $a'$, $\mathbb{E}_{\text{ref}}\{a_k\} = \Delta a_{\text{ref}}/2$, where $\Delta a_{\text{ref}}$ is the minimum distance for the reference system. The expressions in (6.7) and (6.8) hold in general for all finite set of constellation points $\mathcal{C}$.

## 6.2.1   Similar Eye-opening

Initially, we compare the pulses in a noise-free setting. For any Nyquist pulse with a sampling receiver, the minimum eye opening after filtering (see Fig. 6.1) is given

by (6.4) as

$$\min_{a,a'\in\mathcal{C},a\neq a'} |AG(0)\left(\mu + aq(0)\right) - AG(0)\left(\mu + a'q(0)\right)| = AG(0)\Delta aq(0). \qquad (6.9)$$

As a result, to have the same eye opening as with the reference pulse, we require $A_{\mathrm{ref}}/A = \Delta aq(0)/\Delta a_{\mathrm{ref}}$, which substituted into (6.7) yields

$$\Upsilon = 10\log_{10}\left(\frac{\Delta aq(0)}{2\left(\mu + \mathbb{E}\left\{a_k\right\}\overline{q}\right)}\right). \qquad (6.10)$$

Fig. 6.2 demonstrates the comparison of the optical power gain for various pulses defined in Sec. 4.2 for both OOK and 4-PAM formats, where the signals are scaled to have equal eye opening. The S2 pulse (4.6) with OOK modulation, which is used as a baseline for comparison, is shown in the figure with an arrow. The results for SRC and SDJ have been derived before in [9, Fig. 4], whereas the results for other pulses are novel, where $T_{\mathrm{b}} = T_{\mathrm{s}}/\log_2 M$ is the bit rate. OOK is chosen rather than BPSK for compatibility with [9], although these binary formats are entirely equivalent for $BT_{\mathrm{b}} \leq 1$, as shown in Theorem 3. In these examples, we use $\Delta a = \Delta a_{\mathrm{ref}}$; however, rescaling the considered constellation $\mathcal{C}$ would not change the results, as it would affect the numerator and denominator of (6.10) equally.

For the nonnegative pulses in Sec. 4.2.2 (i.e., SRC and SDJ) with OOK, where $\mu = 0$, by increasing the bandwidth, the optical power gain, which depends on $\alpha$ through its dependence on $\overline{q}$, increases since $\overline{q}$ decreases. The results in Fig. 6.2 are consistent with [9, Fig. 4], where the same nonnegative pulses were presented. It can be seen that when the regular Nyquist pulses (RC, BTN, PL, and Poly) are used, and the nonnegativity constraint is satisfied by adding a DC bias, transmission is possible over a much narrower bandwidth. However, since the DC bias consumes energy and does not carry information, the optical power gain will be reduced.
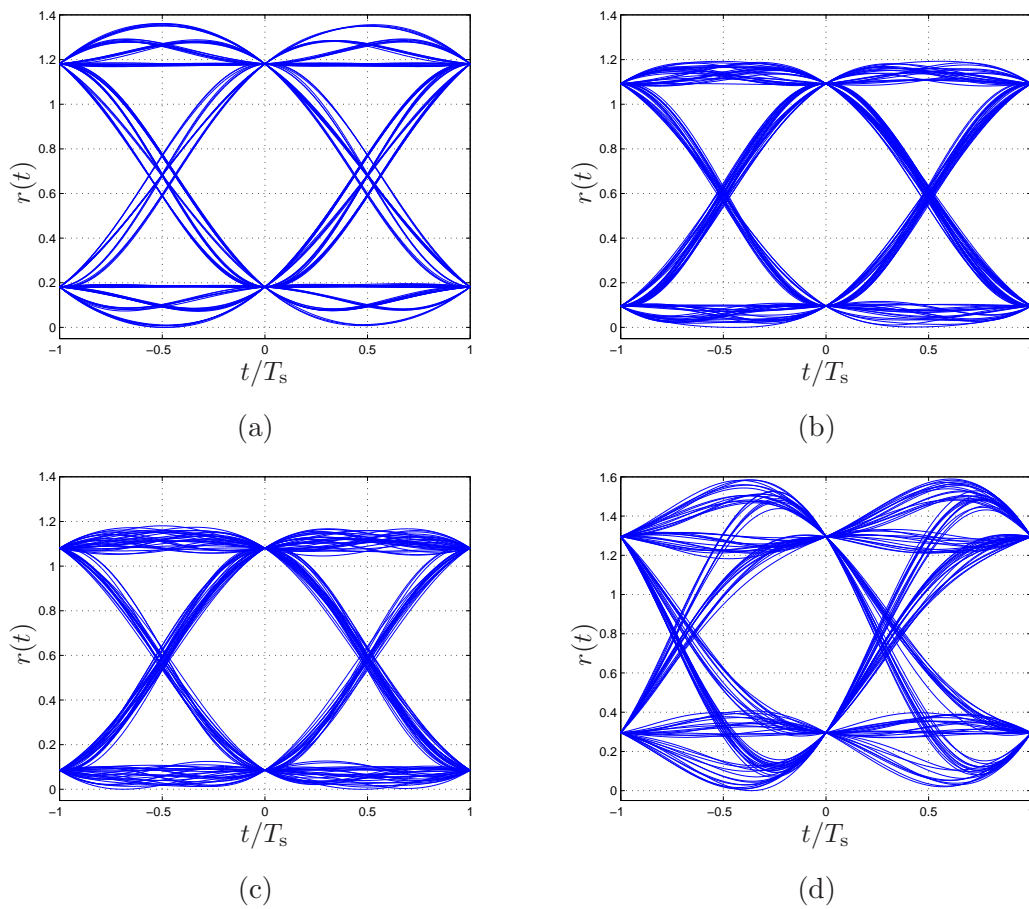
Figure 6.1.   Noise-free eye diagrams for (a) RC, (b) PL, (c) BTN, and (d) Xia pulses with OOK modulation ($\mathcal{C} = \{0, 1\}$) and sampling receiver. All pulses have $\alpha = 0.60$ and are normalized to have the same optical power $\bar{q} = 1$.
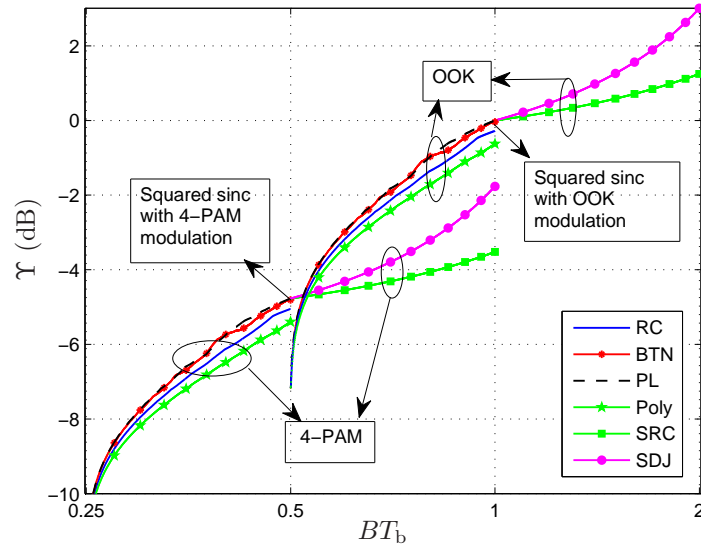
Figure 6.2.    The optical power gain $\Upsilon$ versus normalized bandwidth $BT_b$ for various Nyquist pulses with a sampling receiver. The noiseless eye opening for all pulses is equal. The curves for $BT_b \geq 1$ agree with [9].

There is a compromise between bandwidth and optical power gain, due to the fact that $\mu$ will be reduced by increasing the roll-off factor (see Fig. 5.1), whereas the required bandwidth increases. The highest optical power gain for all pulses will be achieved when the roll-off factor $\alpha$ is one. The reason is that by increasing the roll-off factor, the required bias which is the only parameter in (6.7) that depends on $\alpha$ decreases (see Fig. 5.1). The BTN and the PL pulses have approximately similar optical power gain, and the RC and Poly pulses have smaller gains, due to higher $\mu$, which is also visible in the eye diagrams of Fig. 6.1.

Comparing the binary and 4-PAM cases for the same $\alpha$ and $\Delta a$, we can see in Fig. 6.2 that by using higher-order modulation formats, the optical power gain for all pulses decreases, since in (6.7), $\mathbb{E}\{a_k\}$ and $\mu$ will increase. For $0.5 < BT_b < 1$, the optical power gain for the best 4-PAM system with nonnegative Nyquist pulses is up to 2.39 dB less than the gain of the best OOK system with regular Nyquist pulses. For $0.5 < BT_b < 1$, the optical power gain for the best 4-PAM system with

nonnegative Nyquist pulses is up to 2.39 dB less than the gain of the best OOK system with regular Nyquist pulses.

For any root-Nyquist pulse with a matched filter receiver, the minimum eye opening after filtering is given by (6.6) as

$$\min_{a,a'\in\mathcal{C},a\neq a'} |A\zeta\left(\mu Q(0)+aE_q\right)-A\zeta\left(\mu Q(0)+a'E_q\right)| = A\zeta\Delta aE_q. \qquad (6.11)$$

Since the eye openings in (6.9) and (6.11) depend on the receiver filter gains $G(0)$ or $\zeta$, pulses should be compared using the same receiver filter. In particular, it is not relevant to compare the sampling receiver with matched filters in this context, since the outcome would depend on the ratio $G(0)/\zeta$, which can be chosen arbitrarily. This is the reason why root-Nyquist pulses are not included in Fig. 6.2.

## 6.2.2   Similar SER

It appears from Fig. 6.2 that the studied pulses become more power-efficient when the bandwidth is increased. A higher bandwidth, however, for sampling receiver means that the receiver filter admits more noise, which reduces the receiver performance. In Fig. 6.3, we therefore compare the average optical power gain of Nyquist and root-Nyquist pulses, when the power is adjusted to yield a constant SER equal to $10^{-6}$. Since the amount of noise after the matched filter receiver does not depend on the bandwidth, we considered this fact as a potential advantage, and therefore included root-Nyquist pulses in the following analysis. Similarly to the previous case, the S2 pulse (4.6) with OOK and sampling receiver is used as a baseline for comparison.

So far, the analysis holds for a general $\mathcal{C}$. To find the optical power gain as a function

of SER for the sampling receiver, we first apply a maximum likelihood detector to (6.4), assuming a special case in which $\mathcal{C}$ is an $M$-PAM constellation, which yields the SER [6, Sec. 9.3]

$$P_{\text{err}} = 2\frac{M-1}{M}Q\left(\frac{AG(0)\Delta aq(0)}{2\sqrt{G(0)^2 N_0 B}}\right)$$

where

$$Q(x) = \frac{1}{\sqrt{2\pi}}\int\limits_x^\infty \exp\left(\frac{-x^2}{2}\right)dx$$

is the Gaussian Q-function. As a result,

$$A = \frac{2}{\Delta aq(0)}Q^{-1}\left(P_{\text{err}}\frac{M}{2\,(M-1)}\right)\sqrt{N_0 B}$$

and

$$\frac{A_{\text{ref}}}{A} = \frac{\Delta aq(0)}{\Delta a_{\text{ref}}}\frac{Q^{-1}\left(P_{\text{err}}\right)}{Q^{-1}\left(P_{\text{err}}\frac{M}{2(M-1)}\right)}\sqrt{\frac{B_{\text{ref}}}{B}}, \tag{6.12}$$

where $B_{\text{ref}} = 1/T_{\text{b}}$ is the bandwidth of the reference pulse. The optical power gain now follows from (6.7).

For the matched filter receiver, by applying the maximum likelihood detector to (6.6), the SER will be [6, Sec. 9.3]

$$P_{\text{err}} = 2\frac{M-1}{M}Q\left(\frac{A\Delta a E_q\zeta}{2\sqrt{\frac{\zeta^2 N_0 E_q}{2}}}\right)$$

$$= 2\frac{M-1}{M}Q\left(A\Delta a\sqrt{\frac{E_q}{2N_0}}\right).$$

As a result,

$$A = \frac{1}{\Delta a}Q^{-1}\left(P_{\text{err}}\frac{M}{2\,(M-1)}\right)\sqrt{\frac{2N_0}{E_q}}$$
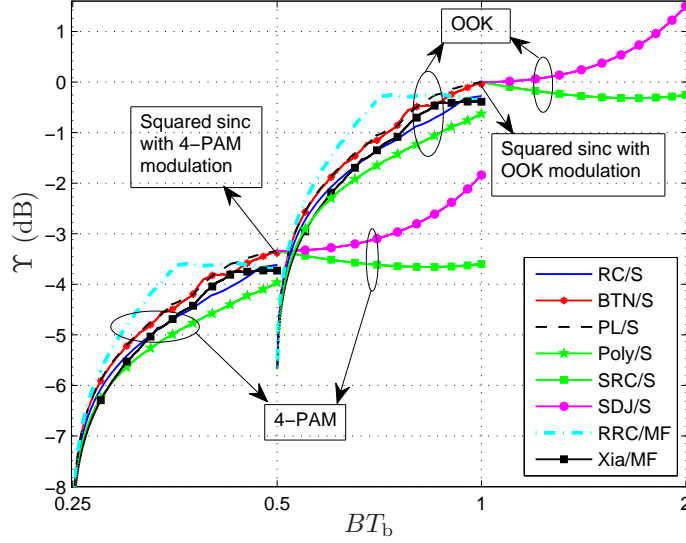
Figure 6.3. The optical power gain versus normalized bandwidth $BT_b$ for various pulses with a sampling receiver (S) or matched filter receiver (MF). The SER for all pulses is $10^{-6}$.

and

$$\frac{A_{\mathrm{ref}}}{A} = \frac{\Delta a}{\Delta a_{\mathrm{ref}}} \frac{\sqrt{2}Q^{-1}\left(P_{\mathrm{err}}\right)}{Q^{-1}\left(P_{\mathrm{err}}\frac{M}{2(M-1)}\right)} \sqrt{E_q B_{\mathrm{ref}}}. \tag{6.13}$$

In contrast to the case with equal eye openings (see Fig. 6.2), Nyquist and root-Nyquist pulses can be compared with each other when the SER is kept constant, since neither (6.12) nor (6.13) depend on the filter gains $G(0)$ and $\zeta$.

By increasing the bandwidth, the gain for SRC decreases slightly, whereas it increases for SDJ, where $\mu = 0$ for both cases. The reason is that for these pulses by increasing $\alpha$, both $\overline{q}$ and the ratio $A_{\mathrm{ref}}/A$ decreases. We observe that for the regular Nyquist pulses in Sec. 4.2.1, the gain increases by increasing the bandwidth. The reason is that by increasing the roll-off factor, the required bias decreases much faster (see Fig. 5.1) than the speed of increase in bandwidth. The BTN and the PL pulses have approximately similar gain, and the gains of the RC and Poly pulses are always smaller than the gain of the other two pulses.

In case of the matched filter receiver, the noise variance does not depend on band-width. As a result, the ratio $A_\mathrm{ref}/A$ (6.13) is not a function of the roll-off factor and the optical power gain only depends on the roll-off factor through its dependence on the required DC bias. In Fig. 6.3, for $0.5 < BT_\mathrm{b} \leq 0.71$, the optical power gain of the RRC pulse increases, and a wide gap is maintained with respect to the Nyquist pulses. For $0.71 < BT_\mathrm{b} \leq 1$, since the required DC is slightly fluctuating, the same happens for optical power gain of RRC, and the maximum optical power gain happens at $BT_\mathrm{b} = 0.86$, where it is $\Upsilon = -0.22$ dB. The Xia pulse has a similar behavior, though it is not better than all Nyquist pulses.

For $\alpha \to 1$, the optical power gain of the Xia, RC, and RRC pulses are approximately equal since the output of matched filter will be equal to an RC pulse by either using the RRC or the Xia pulse. However, the optical power of mentioned pulses will be different for other values of $\alpha$.

By increasing the modulation level from binary to 4-PAM, for the same $\alpha$ and $\Delta a$, the optical power gain for all pulses decreases, since the required DC bias and symbol average increase while the ratio $A_\mathrm{ref}/A$ decreases. For $0.5 < BT_\mathrm{b} < 1$, the optical power gain of the regular Nyquist pulses and root-Nyquist pulses with OOK modulation is significantly higher than the gain for the all nonnegative Nyquist pulses with 4-PAM.

When the roll-off factor is equal to zero (i.e., the normalized bandwidth $BT_\mathrm{b}$ for the biased pulses with binary modulation is equal to 0.5 and for the biased pulses with 4-PAM is equal to 0.25), the regular Nyquist pulses discussed in Sec. 4.2.1 and the root-Nyquist pulses in 4.3 will become equal to a sinc pulse with bandwidth $1/(2T_\mathrm{s})$. As discussed in Chap. 5, the required DC will be infinite for the sinc pulse. Hence, the gain $\Upsilon$ will asymptotically go to $-\infty$ when $\alpha \to 0$.

# 7   CONCLUSION AND FUTURE WORK

In this work, a pulse shaping method for strictly bandlimited IM/DD systems is presented, in which the transmitted electrical signal must be nonnegative. The proposed approach adds a constant DC bias to the transmitted signal, which allows a wider selection of transmitted pulses without violating the nonnegativity constraint. This allows us to use Nyquist or root-Nyquist pulses for ISI-free transmission, with narrower bandwidth compared to previous works. It is possible to transmit with a bandwidth equal to that of ISI-free transmission in conventional coherent channels.

To compare our proposed transmission schemes with previously designed schemes and to see the effect of increasing the modulation level, we evaluated analytically the average optical power versus bandwidth in two different scenarios. The optimization of modulation formats means a tradeoff between the two components of the optical power: the constellation power, which carries the data and is similar to the coherent case, and the bias power, which is constant. We prove the somewhat unexpected results that for narrowband transmission ($BT_\mathrm{s} \leq 1$), the two powers balance each other perfectly, so that OOK and BPSK have identical performance regardless of the pulse.

In the first scenario, the Nyquist pulses are compared when the noise-free eye opening is equal for all the pulses and modulation formats. Of the studied pulses, the SDJ pulse with OOK is the best known, as previously shown in [9] over $BT_\mathrm{b} \geq 1$. At $0.5 < BT_\mathrm{b} < 1$, the PL and BTN pulses with binary modulation have the best performance, being up to 2.39 dB better than SDJ with 4-PAM modulation. Similarly, the 4-PAM BTN and PL pulses have highest gain over $0.25 < BT_\mathrm{b} < 0.5$.

In the second scenario, all pulses have equal SER. Of the studied pulses, the SDJ with OOK modulation and sampling receiver has the highest gain for $BT_\mathrm{b} \geq 1$.

At $0.869 < BT_b < 1$, the binary PL pulse has the best performance, whereas for $0.5 < BT_b \leq 0.869$, the RRC pulse with matched filter receiver achieves the highest gain. For $0.25 < BT_b \leq 0.434$, the 4-PAM system with an RRC pulse has the best performance, while for $0.434 < BT_b \leq 0.5$, the PL pulse has the best performance. The gain of RRC in this scenario is up to 0.74 dB over the best Nyquist pulse and 2.80 dB over the best known results with unbiased PAM.

## 7.1   Suggestions for Future Work

This work can be a starting point for ISI-free pulse shaping design for transmission within a bandwidth equal to that of coherent conventional channels. Future work can concentrate on:

- Designing coding schemes in bandlimited regime, to improve the BER performance and compensate the effect of the DC bias.

- Analyzing the effect of other types of noise on the performance of the designed transmission scheme since in this thesis, the noise was modeled as AWGN. Although, as it was mentioned earlier, this is a good approximation, it does not cover all applications.

- Relaxing the strictly bandlimited condition and conducting research on the application of prolate spheroidal functions on the minimum bandwidth intensity modulation systems.

- Utilizing the most recently proposed Nyquist pulses [13, 16, 18, 66, 67], or their corresponding root-Nyquist pulses, and carefully optimizing their parameters to achieve further improvements in optical power gain.

- Extending to $M$-PAM systems with $M > 4$ to gain more spectral efficiency at the cost of reduced power efficiency.

# Bibliography

[1] S. Randel, F. Breyer, and S. C. J. Lee, "High-speed transmission over multi-mode optical fibers," in *Conference on Optical Fiber communication/National Fiber Optic Engineers Conference (OFC/NFOEC)*, p. OWR2, Feb. 2008.

[2] D. Molin, G. Kuyt, M. Bigot-Astruc, and P. Sillard, "Recent advances in MMF technology for data networks," in *Optical Fiber Communication Conference*, p. OWJ6, Mar. 2011.

[3] F. R. Gfeller and U. Bapst, "Wireless in-house communication via diffuse infrared radiation," *Proceedings of the IEEE*, vol. 67, no. 11, pp. 1474–1486, 1979.

[4] J. M. Kahn and J. R. Barry, "Wireless infrared communications," *Proceedings of the IEEE*, vol. 85, no. 2, pp. 265–298, Feb. 1997.

[5] S. Hranilovic, "On the design of bandwidth efficient signalling for indoor wireless optical channels," *International Journal of Communication Systems*, vol. 18, no. 3, pp. 205–228, 2005.

[6] J. G. Proakis and M. Salehi, *Digital communications*. New York: McGraw-Hill, 4 ed., 2001.

[7] P. Westbergh, J. S. Gustavsson, Å. Haglund, A. Larsson, F. Hopfer, G. Fiol, D. Bimberg, A. Joel, "32 Gbit/s multimode fibre transmission using high-speed, low current density 850 nm VCSEL," *Electronics letters*, vol. 45, no. 7, pp. 366–368, 2009.

[8] B. Inan, S. C. J. Lee, S. Randel, I. Neokosmidis, A. M. J. Koonen, and J. W. Walewski, "Impact of LED nonlinearity on discrete multitone modulation,"

*Journal of Optical Communications and Networking*, vol. 1, no. 5, pp. 439–451, 2009.

[9] S. Hranilovic, "Minimum-bandwidth optical intensity Nyquist pulses," *IEEE Transactions on Communications*, vol. 55, pp. 574–583, Mar. 2007.

[10] R. E. Freund, C. A. Bunge, N. N. Ledentsov, D. Molin, and C. Caspar, "High-speed transmission in multimode fibers," *Journal of Lightwave Technology*, vol. 28, pp. 569–586, Feb. 2010.

[11] H. Nyquist, "Certain topics in telegraph transmission theory," *Transactions of the American Institute of Electrical Engineers*, vol. 47, pp. 617–644, Apr. 1928.

[12] L. E. Franks, "Further results on Nyquist's problem in pulse transmission," *IEEE Transactions on Communication Technology*, vol. 16, pp. 337–340, Apr. 1968.

[13] N. C. Beaulieu and M. O. Damen, "Parametric construction of Nyquist-I pulses," *IEEE Transactions on Communications*, vol. 52, pp. 2134–2142, Dec. 2004.

[14] P. Winzer and R. Essiambre, "Advanced modulation formats for high-capacity optical transport networks," *Journal of Lightwave Technology*, vol. 24, no. 12, pp. 4711–4728, 2006.

[15] E. Ip, A. Lau, D. Barros, and J. Kahn, "Coherent detection in optical fiber systems," *Optics Express*, vol. 16, no. 2, pp. 753–791, 2008.

[16] N. C. Beaulieu, C. C. Tan, and M. O. Damen, "A 'better than' Nyquist pulse," *IEEE Communications Letters*, vol. 5, no. 9, pp. 367–368, Sep. 2001.

[17] S. Chennakeshu and G. Saulnier, "Differential detection of $\pi/4$-shifted-DQPSK for digital cellular radio," *IEEE Transactions on Vehicular Technology*, vol. 42, pp. 46–57, Feb. 1993.

[18] S. Chandan, P. Sandeep, and A. K. Chaturvedi, "A family of ISI-free polynomial pulses," *IEEE Communications Letters*, vol. 9, no. 6, pp. 496–498, June 2005.

[19] G. Forney Jr and L. Wei, "Multidimensional constellations–part i: Introduction, figures of merit, and generalized cross constellations," *IEEE Journal on Selected Areas in Communications*, vol. 7, no. 6, pp. 877–892, 1989.

[20] D. Shiu and J. Kahn, "Shaping and nonequiprobable signaling for intensity-modulated signals," *IEEE Transactions on Information Theory*, vol. 45, no. 7, pp. 2661–2668, 1999.

[21] W. Mao and J. Kahn, "Lattice codes for amplified direct-detection optical systems," *IEEE Transactions on Communications*, vol. 56, no. 7, pp. 1137–1145, 2008.

[22] J. Barry, *Wireless infrared communications*. Kluwer Academic Publishers, 1994.

[23] S. Hranilovic, *Wireless optical communication systems*. Springer, 2005.

[24] S. Hranilovic and D. A. Johns, "A multilevel modulation scheme for high-speed wireless infrared communications," in *Proceedings of the IEEE International Symposium on Circuits and Systems*, vol. 6, pp. 338–341, Jul. 1999.

[25] A. A. Farid and S. Hranilovic, "Capacity bounds for wireless optical intensity channels with Gaussian noise," *IEEE Transactions on Information Theory*, vol. 56, no. 12, pp. 6066–6077, Dec. 2010.

[26] S. Hranilovic and F. R. Kschischang, "Capacity bounds for power- and band-limited optical intensity channels corrupted by Gaussian noise," *IEEE Transactions on Information Theory*, vol. 50, no. 5, pp. 784–795, May 2004.

[27] A. Lapidoth, S. M. Moser, and M. A. Wigger, "On the capacity of free-space optical intensity channels," *IEEE Transactions on Information Theory*, vol. 55, no. 10, pp. 4449–4461, Oct. 2009.

[28] A. A. Farid and S. Hranilovic, "Capacity of optical intensity channels with peak and average power constraints," in *IEEE International Conference on Communications*, Jun. 2009.

[29] R. You and J. M. Kahn, "Capacity bound of optical IM/DD channels using multiple-subcarrier modulation with fixed bias," in *IEEE International Conference on Communications*, pp. 2757–2762, Jun. 2001.

[30] R. You and J. M. Kahn, "Upper-bounding the capacity of optical IM/DD channels with multiple-subcarrier modulation and fixed bias using trigonometric moment space method," *IEEE Transactions on Information Theory*, vol. 48, no. 2, pp. 514–523, Feb. 2002.

[31] H. Sugiyama and K. Nosu, "MPPM: A method for improving the band-utilization efficiency in optical PPM," *IEEE Journal of Lightwave Technology*, vol. 7, pp. 465–472, Mar. 1989.

[32] H. Park and J. Barry, "Modulation analysis for wireless infrared communications," in *IEEE International Conference on Communications*, vol. 2, pp. 1182–1186, 1995.

[33] J. B. Carruthers and J. M. Kahn, "Multiple-subcarrier modulation for nondirected wireless infrared communication," *IEEE Journal on Selected Areas in Communications*, vol. 14, pp. 538–546, Apr. 1996.

[34] S. Hranilovic and F. R. Kschischang, "Optical intensity-modulated direct detection channels: Signal space and lattice codes," *IEEE Transactions on Information Theory*, vol. 49, pp. 1385–1399, Jun. 2003.

[35] J. Karout, E. Agrell, and M. Karlsson, "Power efficient subcarrier modulation for intensity modulated channels," *Optics Express*, vol. 18, no. 17, pp. 17913–17921, 2010.

[36] N. D. Chatzidiamantis, A. S. Lioumpas, G. K. Karagiannidis, and S. Arnon, "Adaptive subcarrier PSK intensity modulation in free space optical systems," *IEEE Transactions on Communications*, vol. 59, pp. 1368–1377, May 2011.

[37] M. D. Audeh, J. M. Kahn, and J. R. Barry, "Performance of pulse-position modulation on measured non-directed indoor infrared channels," *IEEE Transactions on Communications*, vol. 44, no. 6, pp. 654–659, Jun. 1996.

[38] J. Barry, J. Kahn, W. Krause, E. Lee, and D. Messerschmitt, "Simulation of multipath impulse response for indoor wireless optical channels," *IEEE Journal on Selected Areas in Communications*, vol. 11, no. 3, pp. 367–379, 1993.

[39] A. Wiberg, B. Olsson, and P. Andrekson, "Single cycle subcarrier modulation," in *Optical Fiber Communication Conference*, Optical Society of America, 2009.

[40] B. Olsson and A. Alping, "Electro-optical subcarrier modulation transmitter for 100 gbe dwdm transport," in *Asia Optical Fiber Communication and Optoelectronic Exposition and Conference*, Optical Society of America, 2008.

[41] B. Olsson and M. Sköld, "QPSK transmitter based on optical amplitude modulation of electrically generated QPSK signal," in *Asia Optical Fiber Communication and Optoelectronic Exposition and Conference*, Optical Society of America, 2008.

[42] J. Armstrong, "OFDM for optical communications," *Journal of Lightwave Technology*, vol. 27, no. 3, pp. 189–204, 2009.

[43] L. Hanzo, M. Münster, B. Choi, and T. Keller, *OFDM and MC-CDMA for Broadband Multi-user Communications, WLANs and Broadcasting.* John Wiley & Sons, 2003.

[44] S. Teramoto and T. Ohtsuki, "Multiple-subcarrier optical communication systems with subcarrier signal-point sequence," *IEEE Transactions on Communications*, vol. 53, no. 10, pp. 1738–1743, 2005.

[45] O. Gonzalez, R. Perez-Jimenez, S. Rodriguez, J. Rabadan, and A. Ayala, "OFDM over indoor wireless optical channel," in *IEEE Proceedings-Optoelectronics*, vol. 152, pp. 199–204, 2005.

[46] J. Armstrong, B. Schmidt, D. Kalra, H. Suraweera, and A. Lowery, "Performance of asymmetrically clipped optical OFDM in AWGN for an intensity modulated direct detection system," in *IEEE Global Communications Conference*, 2006.

[47] R. You and J. Kahn, "Average power reduction techniques for multiple-subcarrier intensity-modulated optical signals," in *IEEE International Conference on Communications*, vol. 3, pp. 1620–1627, 2000.

[48] N. Kitamoto and T. Ohtsuki, "Parallel combinatory multiple-subcarrier optical wireless communication systems," *International Journal of Communication Systems*, vol. 18, no. 3, pp. 195–203, 2005.

[49] W. Kang and S. Hranilovic, "Power reduction techniques for multiple-subcarrier modulated diffuse wireless optical channels," *IEEE Transactions on Communications*, vol. 56, no. 2, pp. 279–288, 2008.

[50] S. Hranilovic, "Minimum bandwidth Nyquist and root-Nyquist pulses for optical intensity channels," in *IEEE Global Communications Conference*, vol. 3, pp. 1368–1372, Nov.–Dec. 2005.

[51] A. Bhandari, M. Kumar, and M. Trikha, "Squared pulse shaping filters for ISI-free communication in optical intensity channels," in *IEEE Signal Processing and Communications Applications*, 2007.

[52] H. Landau and H. Pollak, "Prolate spheroidal wave functions, Fourier analysis and uncertainty II," *Bell Syst. Tech. J*, vol. 40, no. 1, pp. 65–84, 1961.

[53] J. Cunningham, D. Beckman, X. Zheng, D. Huang, T. Sze, and A. Krishnamoorthy, "PAM-4 signaling over VCSELs with 0.13 $\mu$m CMOS chip technology," *Optics Express*, vol. 14, no. 25, pp. 12028–12038, 2006.

[54] I. Bar-David and G. Kaplan, "Information rates of photon-limited overlapping pulse position modulation channels," *IEEE Transactions on Information Theory*, vol. 30, no. 3, pp. 455–464, 1984.

[55] G. Lee and G. Schroeder, "Optical pulse position modulation with multiple positions per pulsewidth," *IEEE Transactions on Communications*, vol. 25, no. 3, pp. 360–364, 1977.

[56] C. Georghiades, "Some implications of TCM for optical direct-detection channels," *IEEE Transactions on Communications*, vol. 37, no. 5, pp. 481–487, 1989.

[57] K. Abend, "Optimum photon detection (corresp.)," *IEEE Transactions on Information Theory*, vol. 12, no. 1, pp. 64–65, 1966.

[58] B. Reiffen and H. Sherman, "An optimum demodulator for poisson processes: Photon source detectors," *Proceedings of the IEEE*, vol. 51, no. 10, pp. 1316–1320, 1963.

[59] R. Gagliardi and S. Karp, "M-ary poisson detection and optical communications," *IEEE Transactions on Communication Technology*, vol. 17, no. 2, pp. 208–216, 1969.

[60] D. Shiu and J. Kahn, "Differential pulse-position modulation for power-efficient optical communication," *IEEE Transactions on Communications*, vol. 47, no. 8, pp. 1201–1210, 1999.

[61] M. Mohamed and S. Hranilovic, "Optical impulse modulation for diffuse indoor wireless optical channels," in *IEEE International Conference on Communications*, pp. 2140–2145, 2007.

[62] J. M. Kahn, W. J. Krause, and J. B. Carruthers, "Experimental characterization of non-directed indoor infrared channels," *IEEE Transactions on Communications*, vol. 43, no. 2–4, pp. 1613–1623, Feb.–Apr. 2002.

[63] A. Papoulis and S. Pillai, *Probability, random variables and stochastic processes with errata sheet.* McGraw Hill Higher Education, 2002.

[64] D. Gloge and E. Marcatili, "Multimode theory of graded-core fibers," *Bell Syst. Tech. J*, vol. 52, no. 9, pp. 1563–1578, 1973.

[65] G. Agrawal, *Lightwave technology: Telecommunication systems*, vol. 1. Wiley-Blackwell, 2005.

[66] N. D. Alexandru and A. L. Onofrei Balan, "Improved Nyquist filters with piece-wise parabolic frequency characteristics," *IEEE Communications Letters*, vol. 15, no. 5, pp. 473–475, May 2011.

[67] S. D. Assimonis, M. Matthaiou, G. K. Karagiannidis, and J. A. Nossek, "Improved parametric families of intersymbol interference-free Nyquist pulses using inner and outer functions," *IET Signal Processing*, vol. 5, no. 2, pp. 157–163, 2011.

[68] J. Scanlan, "Pulses satisfying the Nyquist criterion," *Electronics Letters*, vol. 28, no. 1, pp. 50–52, 1992.

[69] S. Lee and N. Beaulieu, "A novel pulse designed to jointly optimize symbol timing estimation performance and the mean squared error of recovered data," *IEEE Transactions on Wireless Communications*, vol. 7, no. 11, pp. 4064–4069, 2008.

[70] A. Opperman and L. Linde, "Design considerations and applications of a class of asymmetrically matched Nyquist low pass filters," in *South African Symposium on Communications and Signal Processing*, pp. 166–171, 1991.

[71] G. Turin, "An introduction to matched filters," *IEEE Transactions on Information Theory*, vol. 6, pp. 311–329, Jun. 1960.

[72] D. North, "An analysis of the factors which determine signal/noise discrimination in pulsed-carrier systems," *Proceedings of the IEEE*, vol. 51, no. 7, pp. 1016–1027, 1963.

[73] S. Mneina and G. Martens, "Linear phase matched filter design with causal real symmetric impulse response," *International Journal of Electronics and Communications*, vol. 63, no. 2, pp. 83–91, 2009.

[74] X. G. Xia, "A family of pulse-shaping filters with ISI-free matched and unmatched filter properties," *IEEE Transactions on Communications*, vol. 45, no. 10, pp. 1157–1158, 1997.

[75] T. Demeechai, "Pulse-shaping filters with ISI-free matched and unmatched filter properties," *IEEE Transactions on Communications*, vol. 46, no. 8, p. 992, 1998.

[76] A. Kisel, "An extension of pulse shaping filter theory," *IEEE Transactions on Communications*, vol. 47, no. 5, pp. 645–647, 1999.

[77] N. Alagha and P. Kabal, "Generalized raised-cosine filters," *IEEE Transactions on Communications*, vol. 47, no. 7, pp. 989–997, 1999.

[78] C. C. Tan and N. C. Beaulieu, "Transmission properties of conjugate-root pulses," *IEEE Transactions on Communications*, vol. 52, no. 4, pp. 553–558, 2004.

[79] D. Slepian, "Some comments on Fourier analysis, uncertainty and modeling," *SIAM review*, pp. 379–393, 1983.